**Charles University in Prague**

Faculty of Mathematics and Physics

**Tomáš Novotný**

# Topics in Non-Stationary Dynamics of Adsorbates on Solid Surfaces

Supervisor: Prof. RNDr. Bedřich Velický, CSc.

Consultant: Doc. RNDr. Petr Chvosta, CSc.

Prague, June 2000

Prohlašuji, že jsem svou disertační práci napsal samostatně a výhradně s použitím citovaných pramenů. Souhlasím se zapůjčováním práce.

V Praze dne 15. června 2000 Tomáš Novotný

# Preface

This work was accomplished as the thesis finishing my PhD studies of theoretical physics at the Department of Theoretical Physics of the Faculty of Mathematics and Physics of Charles University in Prague in years 1996–2000. The work was supervised by Prof. RNDr. Bedřich Velický, CSc. The general topic of the non-stationary surface dynamics was gradually more specified and three particular problems, all of them being motivated by the quartz crystal microbalance measurements by J. Krim, were in the course of my studies considered and solved. Due to my long illness over the summer 1998 the work was considerably slowed down and it was finished about a year later than originally expected during my appointment at the Institute of Physics of the Academy of Sciences of the Czech Republic in Prague. I highly acknowledge the hospitality and welcoming approach of the Institute without the help of which the work would be finished even later.

I am indebted to many people for their help with this work. In the first place I would like to thank Prof. RNDr. Bedřich Velický, CSc. for being the supervisor of the thesis and for the stimulating discussions and the help that he provided me with. I also thank the consultant Doc. RNDr. Petr Chvosta, CSc. who introduced me into the problems of the stochastic resonance and resonant activation and with whom I wrote the paper which forms the third part of the thesis. I am grateful to Prof. RNDr. Vladimír Sechovský, DrSc. for his interest in my work and for the support that he provided me with. Last, but definitely not least I thank to my parents, my colleagues Karel Netočný and Igor Medved' and all other close people for their support during my studies and, more importantly, during the hard times of the illness. I thank them all for their invaluable support.

In Prague, 15 June 2000 Tomáš Novotný

# Contents


**1 Introduction** **1**
- 1.1 Overview . . . 1
- 1.2 QCM experiment . . . 3
- 1.3 Concepts of the microscopic theory of friction . . . 4
- 1.4 Structure of the thesis . . . 9

**2 Lattice friction force: drag of adatom by vibrating substrate** **12**
- 2.1 Formulation of the problem . . . 12
- 2.2 Phenomenology . . . 16
  - 2.2.1 Basic definitions and notation . . . 16
  - 2.2.2 Radiation of point dipole into unbound elastic continuum . . . 18
  - 2.2.3 The Green's function for a halfspace . . . 21
  - 2.2.4 Radiation of point surface dipole into halfspace . . . 25
- 2.3 Projection technique – perturbation theory . . . 27
  - 2.3.1 General formalism . . . 27
  - 2.3.2 Solution of the model . . . 29
- 2.4 Concluding remarks . . . 32

**3 Electronic friction force: adsorbates with dispersive interaction** **34**
- 3.1 Introduction to the electronic friction concept . . . 34
- 3.2 Linear response theory . . . 36
  - 3.2.1 Adsorbates with classical charge distributions . . . 37
  - 3.2.2 Adsorbates with quantum-fluctuating charge distributions . . . 40
- 3.3 Review of results . . . 43
- 3.4 Friction above superconducting substrate . . . 46
- 3.5 Concluding remarks . . . 50

**4 Direct methods in non-stationary stochastic problems in surface physics** **52**
- 4.1 Formulation of the problem . . . 52
- 4.2 Comments to Appendix C . . . 54

**5 Conclusions** **56**

**A Phononic Green's function for the half-space** **65**

**B Electronic Sliding Friction of Atoms Physisorbed at Superconductor Surface** **71**

**C Resonant Activation Phenomenon for Non-Markovian Potential-Fluctuation Processes** **73**

# Chapter 1

# Introduction

## 1.1 Overview

The non-stationary dynamics on surfaces is an important topic of the surface science. Interesting phenomena occur on surfaces both at the macroscopic and microscopic scale. Probably the most interesting macroscopic phenomenon as for the macroscopic dynamics of surfaces is friction. The phenomenological laws of the macroscopic friction force between two bodies sliding relative to each other were found by G. Amontons and Ch. A. Coulomb in the 17th and 18th century. The first law says that the friction force between two flat surfaces is proportional to the normal load, or the force that squeezes the surfaces together. The second one claims that the friction force is independent of the apparent area of the contact. No matter what this area is, the friction force is constant for a constant normal load. The third law states the independence of the friction force on the velocity of the relative movement of the bodies once the motion starts.

These laws are strikingly universal but also surprisingly counterintuitive, namely the independence of the friction force of the contact area of the sliding surface and of the velocity of the movement. In spite of its technological importance, not much progress was done in the fundamental friction theory until the middle of this century. To that time the first wave of the interest in the fundamentals of the friction dates back. The role of the surface roughness was clarified. Surprisingly enough, the surface roughness was ruled out as a mechanism for the friction, but, at the same time, it showed to be crucial for the explanation of the counterintuitive features of the laws of friction. Thanks to the surface roughness the real and the apparent contact area differ in orders of magnitude and the friction force is in fact proportional to the *real area* of the contact. Moreover, it turned out that the real area is proportional to the normal load. Thus, the first two phenomenological laws of friction follow. Surface roughness also helps to understand the third law. One would expect the friction force to be proportional to the sliding velocity. This corresponds to the linear

response regime. The fact that the real friction force is velocity-independent means that the macroscopic friction experiments are not performed in the linear response regime. The reason for that can be in dynamical instabilities as shown already by Tomlinson in 1929. The rapid dynamics (*stick-slip motion*) of the *asperities* due to the surface roughness is a possible explanation of the *elastic instability* responsible for the velocity-independent friction force.

Such was the level of understanding of the fundamental friction processes in the fifties [1]. However, the standalone mechanism of the friction was not known. Since most of the experiments were performed on metallic samples (motivated by the industry) which undergo substantial wear, the conclusion about the microscopic origin of the friction force was that the surfaces are continuously being worn away by the adhesive bonding between them. Little progress in the fundamental studies of sliding friction was made from 1960 till the eighties when a second real burst of theoretical interest into these problems came. The advances of the experimental techniques like the *surface force apparatus* by J. N. Israelashvili, the *friction force microscopy* which is a modification of the scanning tunnelling microscopy, or the *quartz crystal microbalance* by J. Krim and A. Widom together with the progress in computational techniques started the intense exploration of the friction phenomena at various scales, ranging from the macroscopic to the atomic one. There were performed the experiments without wear with a non-zero friction force. The question about the origin of the friction force arose again.

The experiments mentioned above enables to measure the friction force in the wear-free setups at different length scales. The surface force apparatus may be considered to be a macroscopic experiment which reproduces the classical sliding block experiments by Amontons and Coulomb under exactly defined conditions, the friction force microscopy measures the friction force between a tip and the substrate at the mesoscopic length of the order of hundreds of angstrőms, and the quartz crystal microbalance (QCM) experiment probes the friction force between the substrate and an adsorbate layer of the monolayer (or even less) thickness. The different experiments reveal different realms of the friction phenomena. The theory of friction split into several streams according to the particular subject under study which live almost independently [2]. Of course, the results of the microscopic studies may serve as input for the mesoscopic and macroscopic ones.

In this study, we will deal exclusively with the microscopic friction theory which describes the sliding motion of adsorbate layers or even isolated atoms and molecules above specified atomically flat substrate surfaces. The experimental data to such studies are provided by the QCM experiment by J. Krim et al. This branch of the friction theory was called by Krim the *nanotribology*. A nice article about its origin and the problems under study was written by Krim in the Scientific American [3]. This new and rapidly developing field is rich of novel experimental results and unanswered theoretical questions. Even though the experiments are interesting in

themselves, they also lead to the considerations and developments of theoretical concepts outreaching just this experimental field.

## 1.2 QCM experiment

In this section, we will briefly describe the QCM experiment by J. Krim which is used for measurements of the microscopic friction force between the substrate and the adsorbate layer. The QCM technique was used for years for microweighing purposes [4] and was extended by Krim and Widom [5, 6] in the late eighties for the friction measurements.

The schematic picture of the QCM experimental setup is depicted in Fig. 1.1. On a quartz crystal cleaved so as to vibrate in a strictly shear mode with respect to its surface there are evaporated metal electrodes usually made of silver, gold, or lead. One of the electrodes serve as the substrate for the molecularly thin adsorbate layer deposited on its outer surface. By applying an alternate voltage to the electrodes the quartz crystal which is piezoelectric starts to laterally vibrate with a characteristic frequency $\omega_d \approx 10^7 s^{-1}$ and with an amplitude of the order of 100 Å. In the electric circuit driving the microbalance it is possible to measure the resonance curve of the whole electro-mechanical system. One can measure the resonant frequency as well as the damping (or equivalently the quality factor) of the microbalance without and with the adsorbate layer. Upon the adsorption of the layer both the resonant frequency and the quality factor are changed. The change of the resonant frequency corresponds to the change of the mass of the whole microbalance and this information is used for the microweighing of tiny amounts of adsorbate (fraction of a monolayer). The change of the quality factor is caused by slipping of the film with respect to the substrate. With this slipping there is connected the friction force between the adsorbate and substrate which causes additional dissipation of the whole system detected by the change of the quality factor.

The customary interpretation of the QCM experiments assumes the linear (in relative velocity) friction force between substrate and film [5, 6, 2] (linear response regime), but there are also theoretical methods proposed [7] to interpret QCM experiments when the friction is non-linear and there have been QCM friction measurements which give nonlinear friction. Within the customary interpretation the adsorption of the film leads to the shift of the resonant frequency and change in the damping which are related by [6]

$$\frac{\Delta\gamma}{\omega_d} = -2\Delta\omega_d\tau \ , \tag{1.1}$$

where $\omega_d, \Delta\omega_d, \Delta\gamma$ are the resonant frequency, its change upon the adsorption and the change of damping constant, respectively and where $\tau$, the crucial output from

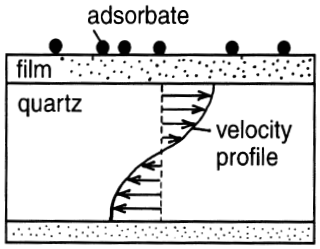


Figure 1.1: A schematic picture of the QCM experiment. A quartz-crystal is vibrating in a strictly shear mode with the velocity profile shown. The films evaporated on it serve as electrodes which drive the piezoelectric oscillations and as a substrate for the adsorbed layer at the same time. From [2].

the experiment, is the so called slip time which yields the relaxation time of the velocity of a free film above the substrate $\vec{v}(t) = \vec{v}_0 e^{-\frac{t}{\tau}}$. The value of $\tau$ is given simply as the inverse of the linear sliding friction coefficient $\eta$ of the adsorbate-substrate interface per unit mass of the adsorbate (surface density $\varrho_2$)

$$\eta = \frac{\varrho_2}{\tau} \ . \tag{1.2}$$

It is the task of the theory or simulations to calculate the friction coefficient $\eta$ measured by the QCM experiment. We will discuss the techniques used to accomplish this task in the next section.

## 1.3 Concepts of the microscopic theory of friction

It is of importance from the theoretical as well as experimental point of view to check the experimental findings and assumptions used to the interpretation of the QCM experiments by an analytical calculations or numerical simulations. Since the many-body problem involved in the truly microscopic description of the experiment is very hard to deal with the simulations are used more often. However, there are already many theoretical results obtained for simplified models which are relevant also for the interpretation of the QCM experiment. In principle, the solution of the model describing the QCM experimental setup needs to give the linear sliding friction coefficient $\eta$ (or, equivalently,the slip time $\tau$) for the film motion above a specified substrate. To this end one has to find the effective equation of motion for the film. This is done by using one of the various *projection techniques* which project out the substrate degrees of freedom and yield the effective motion of the adsorbed film only.

Let us briefly review some of these techniques which can be used to the determination of the microscopic dynamics of adsorbed films. The list of possible methods reads

**Phenomenology** This approach uses heuristic arguments and physical insight to evaluate the desired quantities. As an example we may mention the determination of the friction coefficient from the energy balance considerations.

**Linear response** This is a perturbation method in which the motion of the adsorbate is a prescribed function of time and the response of the substrate to the adsorbate movement is studied in the first order of the perturbation theory. This method is sufficient to evaluate the friction coefficient but cannot clearly give the effective equation of motion of the adsorbate.

**Partitioning** The partitioning method is a fully quantum-mechanical method to find the effective equations of motion for selected quantities. It consist in applying the partitioning scheme to the quantum Liouville equation. It can be done perturbatively or a progressive partitioning scheme may be used leading to the famous Mori continued fraction formalism.

**Exact diagonalization** Some models of the adsorbate-substrate interaction can be solved exactly. These are essentially only the models with the Hamiltonians quadratic in fields involved. An example is the class of models considered by Caldeira and Leggett. The availability of the exact solution in these model is very convenient as different used approximations may be tested against this exact solution. On the other hand, the class of exactly solvable models is rather restricted.

**Non-equilibrium Green's functions** This technique has the advantage that it allows for a systematic perturbation theory in terms of well-known Feynman diagrams. Formally the technique behaves the same as the equilibrium theory and the same approximation schemes can be used.

**Quantum Langevin equation** In this method the effect of the substrate on the adsorbate equation of motion is described by the deterministic friction force and the stochastic noise force. The evolution of the adsorbate is then due to the indeterministic effective behaviour of the substrate (which acts as a reservoir) *stochastic* and the relevant quantities are obtained by averaging over the random variables. The classical example is the well-known Brownian motion.

Some of these methods will be explicitly illustrated in the next. Now, however, we will present the effective description of the adsorbate layer motion in terms of

the generalized Brownian motion model proposed by Persson to simulate the QCM experiment [2] (see also [8]). This model is an *ad hoc* model of the effective equation of motion of the adsorbate in terms of the quantum Langevin equation method. It corresponds to the high temperature limit of the QLE which reduces to the classical one. The equations of motion for the individual particles of the adsorbed film with the coordinate $\vec{r}_i$ read

$$m\frac{d^2\vec{r}_i}{dt^2} + m\overleftrightarrow{\gamma}\cdot\frac{d\vec{r}_i}{dt} = -\nabla_{\vec{r}_i}U - \nabla_{\vec{r}_i}V + \vec{f}_i(t) + \vec{F}_{\rm ext}(t)\ , \tag{1.3}$$

where $m$ denotes the mass of the adsorbate atoms/molecules, $\vec{F}_{\rm ext}(t)$ is the external driving of the film caused by the inertial force due to vibrations of the microbalance, $U = \sum_i u(\vec{r}_i)$ is the adsorbate-substrate potential and $V = \frac{1}{2}\sum'_{i,j} v(\vec{r}_i - \vec{r}_j)$ is the adsorbate-adsorbate interaction potential. The last two quantities are the dynamical effects caused by the interaction with the substrate. The Langevin stochastic (noise) force $\vec{f}_i(t)$ and the linear friction tensor $\overleftrightarrow{\gamma}$ results from the dynamics of the substrate which has been projected out of our effective description. For the substrate in thermal equilibrium, which is not strictly speaking the case of the QCM experiments due to the vibrations, the two quantities are not independent but they are related by the *fluctuation-dissipation theorem*

$$\left\langle \vec{f}_i(t)\vec{f}_j(0)\right\rangle = 2mk_BT\overleftrightarrow{\gamma}\delta_{ij}\delta(t)\ . \tag{1.4}$$

This relation is approximately valid even in the true QCM setup as the non-equilibrium effects due to the acceleration are rather weak.

The equation (1.3) is in the basis of the numerical simulations of the QCM experiment. There are several inputs into the simulation. The interaction potentials $U, V$ can be assessed from the static properties of the adsorbate-substrate system while the dynamic information enters through $\overleftrightarrow{\gamma}$. Already the static properties of the adsorbate-substrate system are non-trivial since several surface phases of the adsorbate may be formed. The dynamical properties are even more complicated. The dependence of the linear sliding friction coefficient or the slip time of the adsorbate film is studied under various conditions including the different surface phases, temperatures, etc. The importance of the input parameter $\overleftrightarrow{\gamma}$ in the simulations is indeed the subject of discussions [8] but it seems that in many cases the measured friction coefficient $\eta$ (inferred from the slip-time) is just equal or very close to the linear friction coefficient $\overleftrightarrow{\gamma}$. Thus, a realistic value for this parameter would surely facilitate the interpretations of the numerical simulations. Therefore, one of the aims of the theorist is to provide a reasonable guess for this quantity.

The microscopic linear friction coefficient $\overleftrightarrow{\gamma}$ describes the dissipative part of the effective action of the substrate on the individual adsorbate atoms. Its microscopic origins are in the dissipation of the thermal energy caused by the adsorbate movement into the substrate degrees of freedom. There are in principle two channels in

which the energy in the substrate is dissipated. The first channel is dissipation into the phononic degrees of freedom — vibrations of the substrate atoms. This mechanism is present for all kinds of surfaces. The second channel is the dissipation into the electronic degrees of freedom — electron-hole pairs or plasmons. This second mechanism is active only for metallic surfaces since for insulating ones the mechanical energy of the adsorbate movement is insufficient to create the excitations over the gap. As the theoretical models usually deal with either of the two mechanisms it would be helpful for the check of their predictions as well as from the practical point of view to know experimentally the relative contributions from the respective channels. The experimental methods that yield the evidence about microscopic linear friction coefficient of an adatom above a specified substrate are beside the QCM also the infra-red spectroscopy and inelastic He scattering but all of them measure the sum of both contributions only.

There have been two suggestions so far how to distinguish experimentally the two dissipative contributions. Persson [9, 10, 2] came up with the idea of the relation between the electronic part of the friction and the surface resistivity. According to him there is direct connection due to the Galilean invariance between the electronic contribution to the friction force and the change of the resistivity of a metallic sample upon the adsorption of the adsorbate layer. From the *surface resistivity measurements* the value of the *electronic friction coefficient* can be calculated. We follow Persson in the argumentation that the movement of the adsorbate over the substrate with the velocity $-\vec{v}$ is from the electronic dissipation point of view equivalent with the stationary adsorbate above the substrate in which the electronic current $\vec{J} = ne\vec{v}$ flows, see Fig. 1.2. The dissipated powers in both these cases are

$$\begin{aligned} P^{\mathrm{el}}_{\mathrm{friction}} &= N_1 m \gamma^{\mathrm{el}} \vec{v}^2 \ , \\ P^{\mathrm{el}}_{\mathrm{current}} &= Ad\Delta\rho \vec{J}^2 \ , \end{aligned} \tag{1.5}$$

where $N_1$ is the number of the adsorbate atoms in the adsorbed film, $m$ is adatom mass, $\gamma^{\mathrm{el}}$ is the electronic part of the friction coefficient, and $-\vec{v}$ is the adsorbate velocity while $A$ is the surface of the substrate covered by the adsorbate, $d$ is thickness of the substrate, $\Delta\rho$ is the change of the substrate resistivity upon the adsorption of the adsorbate (surface resistivity), and $\vec{J}$ is the electric current flowing through the substrate. From the Galilean invariance the dissipation should be in both cases the same which yields by equating the two dissipation powers and taking into account that $\vec{J} = ne\vec{v}$

$$\gamma^{\mathrm{el}} = \frac{n^2 e^2 d}{m n_a} \Delta\rho = \left. \frac{n^2 e^2 d}{m} \frac{\partial \rho}{\partial n_a} \right|_{n_a = 0} \ , \tag{1.6}$$

with $n_a = \frac{N_1}{A}$ being the surface adsorbate density. Thus, the electronic friction coefficient is expressed via the slope of the resistivity change with the adsorbate density

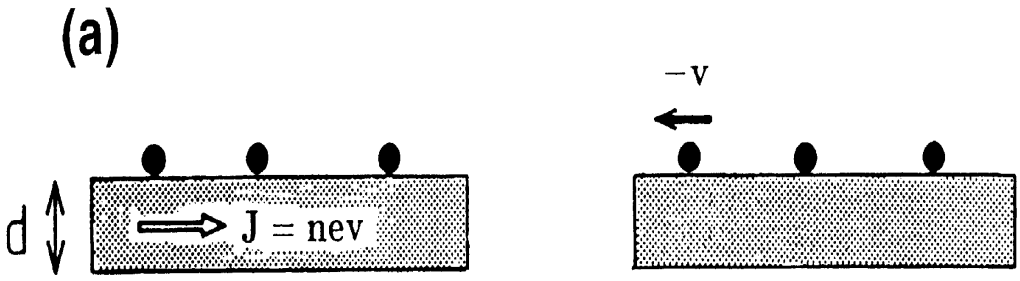


Figure 1.2: A schematic picture of the surface resistivity argument by Persson. The Galilean invariance enables to relate the dissipation due to the surface resistivity change with that due to the moving adsorbate layer. From [2].

for small density. An interesting check mentioned by Persson is that for $d$ sufficiently large (not atomically thin) the electronic friction coefficient is expected to be independent of the thickness of the substrate, i. e. independent of $d$. Therefore, the derivative $\frac{\partial \rho}{\partial n_a}\Big|_{n_a=0}$ should scale like $\frac{1}{d}$ which is indeed observed. This supports the validity of these considerations. On the other hand, the whole method is somewhat controversial and, indeed, there was a debate over it [11, 12] which was not, unfortunately very productive. Finally, it turns out that the method using the heuristic Galilean invariance arguments is approximately correct and the results predicted by it should be within an order of magnitude correct. Sokoloff [13] simulated the Galilean invariance by the explicit calculations for a jellium model with the result that up to a directional factor of the kind of an average of the cosine of the scattering angle the Galilean invariance argument is correct. The surface resistivity method thus enables to roughly assess the importance of the electronic contribution to the microscopic friction. The experiments have been done for various systems, however, it cannot be effectively applied to all systems as the resolution of the resistivity measurements is not always sufficient.

The second suggestion concerning the separation of the electronic versus phononic contributions to the friction force was made by Krim [14] in 1998. Krim et al. measured the friction force of an adlayer made from $N_2$ molecules above the lead substrate. The lead substrate was cooled below the superconducting transition temperature and a sudden drop in the measured friction coefficient was observed (cf. Fig. 1.3). The natural interpretation of this result is that the electronic degrees of freedom decoupled and the electronic contribution to friction was switched off. If this experiment and the interpretation were correct there would be a method how to directly measure the electronic friction coefficient above the metallic substrates which can be made superconducting. However, this experiment has not been repro-

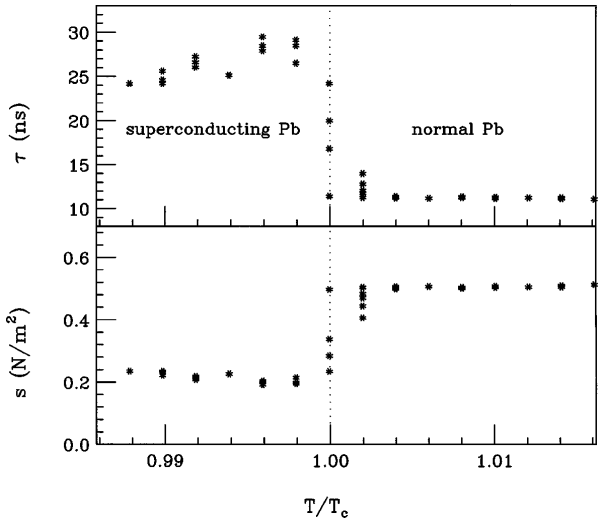


Figure 1.3: The QCM experiment with superconducting friction by Krim et al. Slip time $\tau$ and shear stress $s = \eta v$ (for $v = 1$ cm/s) versus $T/T_C$. The shear stress for nitrogen sliding over the superconducting lead surface is about half that associated with sliding over lead in its normal phase. From [14].

duced yet and the natural interpretation introduced above was contested by Persson and Tosatti [15]. The theoretical arguments of Persson and Tosatti has been refuted by several works and the experiment itself, although not reproduced so far and contested too [16], has not been proven incorrect. The issue still remains open. A part of this work is devoted to the discussion of the superconducting friction force and surveys the contribution made by the author to this question.

Another inspiration from the QCM experiment for the theorist is in the exact analytical solutions of the Langevin equations of the kind presented above. Again, the knowledge of the exact solution in more simple cases may be a check for more complicated simulations. The exact solution of the many-body stochastic problems represented by the above Langevin equation is unfortunately beyond the reach, but even the one-particle cases may exhibit highly non-trivial and physically interesting behaviour. For example, the motion in the periodically tilted wash-board-like potential shows the features of the phenomenon called *stochastic resonance*. Thus, the new developments of the stochastic techniques may be initiated by or, on the other hand, may be relevant for the surface diffusion problems.

## 1.4 Structure of the thesis

The facts presented so far were inspiration for the formulation of the following three problems which are the subject of this thesis.

*In the second chapter*, an exactly soluble model of the phononic contribution to the friction is presented. A similar model was already used by Persson and Rydberg [17] for studies of the vibrational damping of molecules above metallic substrates and also by Georgievskii et al. [18] for the studies of the surface diffusion. In the model, the interaction of an adatom adsorbed on the surface in a minimum of a washboard-like potential is approximated by the harmonic oscillator interacting with the local phononic coordinate on the surface of the substrate. Compared with the other models, we also include driving in order to better describe the QCM setup which is modeled by a driven shifting of the bottom of the harmonic potential well. Two methods of the solutions are employed.

In the first section, we present the formulation of the problem which includes the choice of the Hamiltonian and the discussion of the equivalence between various forms of it in different reference frames related by canonical calculations. In the second section, the microscopic phononic friction coefficient is evaluated using simple phenomenological arguments and in the third section the effective equation of motion of the adatom is found by employing the perturbative projection technique. The second method only refines the phenomenological results which are basically correct. Within the calculation the main ingredient is the retarded Green's function of the phonon field at the interaction site. The evaluation was done with help of the surface Green's functions technique and is presented in Appendix A. Our method of evaluation is different from the ones used by Persson and Georgievskii who used the eigen-modes method. Moreover, a tricky approach of the evaluation of the phononic Green's function motivated by the surface Green's functions technique was used, which is to our knowledge unpublished so far. The concluding remarks to this chapter are in the last section.

*In the third chapter*, there is a review of the current works on the electronic part of the friction force for physisorbed adsorbates. For the physisorption kind of the adsorption bond the binding force may be split into the attractive van der Waals part due to the quantum fluctuations of the adsorbate and substrate charge densities and the repulsive Pauli part due to the quantum mechanical repulsion of the overlap of these densities (Pauli exclusion principle). With both these parts of the binding force there must be associated a dissipative component when the adsorbate is in relative motion to the substrate. It is believed, that the dissipative force consists of two separate components in the same way as the binding force and only the dissipative force associated with the van der Waals part is usually considered. The part associated with the Pauli repulsive force is scarcely modeled by the hard-sphere scattering. Therefore, we present the theory of the van der Waals friction only. A unifying approach within the framework of the linear response theory is presented which encompasses the results of most of the works on the van der Waals friction of adsorbate layers.

After a brief introduction into the whole concept of the electronic friction and

the identification of the only component considered in the first section, we introduce the linear response theory for both the classical adsorbate charge distributions (the ionic bond) and quantum-fluctuating adsorbate charge distributions (the true van der Waals bond) in the second section. We briefly review several recent results on the same topic found in literature and we show connection with our approach in the third section. In the fourth one, the problem of the friction above a superconducting surface introduced above is explored in more detail. The debate initiated by Persson and Tosatti is reviewed and a possible explanation by the author is given. Also other suggestions by other authors to resolve the superconducting friction puzzle are mentioned as well as the reply by Persson which moves this still open question further to the microscopic theory. The concluding remarks are again presented in the last section. In Appendix B we reprint the published paper by the author on the topic of the superconducting friction.

*In the fourth chapter*, an abstract model motivated by the QCM experiment and surface diffusion problems is introduced and resolved. The model exhibits the stochastic phenomenon called the *resonant activation*. This phenomenon is closely related to the stochastic resonance. From a broader point of view in both these phenomena the diffusion in a nontrivial potential profile with barriers, sinks, etc., is considered. Moreover, another "noise" (except for the one causing the diffusion) is always present. This additional noise makes the problem being out of thermodynamic equilibrium. Models out of equilibrium may exhibit interesting features. In the cases of resonant activation and stochastic resonance it is a nontrivial dependence on the parameters of the additional noise. Namely, the generalized transport properties (probability current in a washboard potential or escape rate into a sink) have non-monotonic behaviour with respect to the switching rate of the additional noise. This behaviour indicates a subtle correlation between the transport phenomena and the additional noise. Phenomena of this kind are presently under intensive studies.

In the first section, we give the formulation of the problem. We explain the motivation leading to its formulation and show the interesting physical features which the model exhibits and for which it is being considered. In the second section, the comments to the solution of the problem are summarized. The distinctive features of our solution are compared with the so far known results. In Appendix C we present the preprint form of the paper in which the actual solution of the model is presented. The paper has been submitted to Phys. Rev. E.

*The last chapter* contains the conclusions with the summary of obtained results and the outlook of possible further developments of the problems considered in the thesis.

# Chapter 2

# Lattice friction force: drag of adatom by vibrating substrate

## 2.1 Formulation of the problem

In this chapter, we present the study of the phononic component of the friction of an adatom harmonically pinned above the oscillating substrate. This model, close to the one by Persson and Rydberg[1] [17] and also by Georgievskii et al. [18], will be solved by two different methods, yielding more or less equivalent results.

Let us first specify the Hamiltonian of the model. It corresponds to the dynamics of a single adatom which is harmonically pinned above the semi-infinite substrate approximately described by the elastic continuum theory. The substrate is assumed to fill the halfspace $z \leq 0$, all its dynamical degrees of freedom are supposed to be encompassed in the continuous phononic field, i. e. we omit the electronic degrees of freedom, and this phononic field is taken in the harmonic approximation (up to quadratic terms of the phonon field in the Hamiltonian only). The oscillations of the substrate like in the QCM experiment are simulated by the driving term which shifts the bottom of the pinning potential well in the prescribed oscillatory manner. Thus, the Hamiltonian reads $\hat{H}(t) = \hat{H}_{\mathrm{sub}} + \hat{H}_{\mathrm{ads}}(t) + \hat{H}_{\mathrm{int}}(t)$, where

$$\hat{H}_{\mathrm{sub}} = \sum_{i,j=1}^{3} \int_{z\leq 0} d^3\vec{r} \left( \frac{\hat{\Pi}_i^2(\vec{r})}{2\varrho} + \frac{\lambda}{2} \frac{\partial \hat{u}_i(\vec{r})}{\partial x_i} \frac{\partial \hat{u}_j(\vec{r})}{\partial x_j} + \frac{\mu}{2} \frac{\partial \hat{u}_i(\vec{r})}{\partial x_j} \frac{\partial \hat{u}_i(\vec{r})}{\partial x_j} + \frac{\mu}{2} \frac{\partial \hat{u}_i(\vec{r})}{\partial x_j} \frac{\partial \hat{u}_j(\vec{r})}{\partial x_i} \right) \tag{2.1a}$$

is the Hamiltonian of the harmonic substrate with $\varrho$ being the mass density of the substrate, $\lambda, \mu$ the elastic constants (the Lamé coefficients) and $\hat{u}_i(\vec{r})$ and $\hat{\Pi}_i(\vec{r})$ the

[1] Our model is equivalent to the Persson's one except for the driving term corresponding to the oscillations of the substrate. However, due to the harmonic approximation used for the description of the substrate phononic degrees of freedom, the results for the friction coefficient are the same in both.

conjugated coordinates and momenta of the phonon field, respectively. The other two parts of the Hamiltonian are given by

$$\hat{H}_{\rm ads}(t) + \hat{H}_{\rm int}(t) = \sum_{i=1}^{3} \Big( \frac{\hat{p}_i^2}{2m} + \frac{m\omega_{ii}^2}{2} \left( \hat{x}_i - \hat{u}_i(0) - u_i^d(t) \right)^2 \Big) \ , \tag{2.1b}$$

$$\hat{H}_{\rm ads}(t) = \sum_{i=1}^{3} \Big( \frac{\hat{p}_i^2}{2m} + \frac{m\omega_{ii}^2}{2} \left( \hat{x}_i - u_i^d(t) \right)^2 \Big) \ , \tag{2.1c}$$

$$\hat{H}_{\rm int}(t) = \sum_{i=1}^{3} \Big( \frac{m\omega_{ii}^2}{2} \, \hat{u}_i(0)^2 + m\omega_{ii}^2 \left( u_i^d(t) - \hat{x}_i \right) \hat{u}_i(0) \Big) \ . \tag{2.1d}$$

We have denoted by $m$ the mass of the adatom, $\hat{x}_i$ and $\hat{p}_i$ are its conjugated coordinates and momenta, respectively, and $\omega_{ij}^2$ is the pinning potential frequency tensor whose form is assumed to be $\omega_{ij}^2 = \mathrm{diag}(\omega_\parallel^2, \omega_\parallel^2, \omega_\perp^2)$.

The vector $\vec{u}_d(t) \equiv \vec{u}_d(\vec{r} = 0, t)$ denotes the c-number coordinate of the driven phonon mode at the site where the coupling to the adparticle takes place, i. e. at $\vec{r} = 0$. It is this term which is responsible for the explicit time-dependence of these two parts of the Hamiltonian. In the QCM experiment, the driving term is caused by a macroscopically populated long-wavelength phononic mode with the polarization lateral to the substrate surface. Within the harmonic description of the substrate, we may freely consider this mode to be classical (c-number nature in the Hamiltonian), while all the other modes are taken quantum-mechanically and, moreover, their statistical distribution may be taken as the equilibrium (thermal) one. This approach is a complete analogy to the decomposition of the laser field into a classical laser mode and the quantum rest in QED. This step is, strictly speaking, only allowed when the corresponding field is harmonic. In the case of the unharmonicity, the interaction between modes should be considered.

It is possible to transform this Hamiltonian into other, equivalent, and for some calculations more convenient forms. Such transformed forms may also be often found in the literature. The transformations consists in changing the reference frame to the system co-moving with the bottom of the potential well. It is in fact a series of the Galilean transformations to the reference frames with respect to which the potential well is at rest at each moment. We achieve this transformation by the change of variables $\vec{x}(t) \to \vec{x}(t) - \vec{u}_d(t)$. This choice obviously simplifies the adatom and interaction part of the Hamiltonian (2.1b).

To accomplish this change of variables formally at the quantum mechanical level, we look for a canonical transformation which simplifies the interaction in the desired way. We will work in the Schrődinger picture in the following derivation. An exhaustive discussion of the formulation of the quantum mechanics in generally non-inertial frames of reference together with the relation to different quantum-mechanical pictures may be found in [19].

We consider an arbitrary time-dependent canonical transformation realized by a unitary operator $\hat{S}(t)$ which transforms the quantum-mechanical operators as

$$\hat{A} \to \hat{S}(t)\,\hat{A}\,\hat{S}^{\dagger}(t) \tag{2.2}$$

and the states as

$$|\psi(t)\rangle \to \hat{S}(t)|\psi(t)\rangle\ . \tag{2.3}$$

Thus, this canonical transformation conserves all matrix elements as is required. Taking into account that $|\psi(t)\rangle = \hat{U}(t)|\psi(t_0)\rangle$ with the evolution operator $\hat{U}(t)$ generated by the Hamiltonian (2.1), we may identify the effective evolution operator connected with the transformed operators. Namely,

$$\hat{\mathcal{U}}(t) = \hat{S}(t)\,\hat{U}(t) \tag{2.4}$$

governs the evolution of the transformed operators (2.2). Differentiating (2.4) and employing the Schrődinger equation for $\hat{U}(t)$, we come to the effective Hamiltonian in the transformed "reference frame" determined by the canonical transformation, which is

$$\hat{\mathcal{H}}(t) = \hat{S}(t)\,\hat{H}(t)\hat{S}^{\dagger}(t) + i\hbar\frac{d\hat{S}(t)}{dt}\hat{S}^{\dagger}(t)\ . \tag{2.5}$$

The "anomalous" term containing the time derivative must be present in those cases when the operator generating the canonical transformation explicitly depends on time. In order to simplify the interaction part of the Hamiltonian in the way described above, we have to find the canonical transformation which transforms $\hat{\vec{x}}$ into $\hat{\vec{x}}+\vec{u}_d(t)$, i.e. we are looking for an operator $\hat{S}(t)$ such that $\hat{S}(t)\hat{\vec{x}}\hat{S}^{\dagger}(t) = \hat{\vec{x}}+\vec{u}_d(t)$. There is a whole class of such operators, and they are given by

$$\hat{S}(t) = \exp\Big(\frac{i}{\hbar}\hat{\vec{p}}\cdot\vec{u}_d(t)\Big)\,f(\hat{\vec{x}}) \tag{2.6}$$

with $f(\hat{\vec{x}})$ being a unitary operator composed of the position operators $\hat{\vec{x}}$.

There are two customary choices that can be found in the literature. The first one takes $f(\hat{\vec{x}}) = \hat{1}$, which leads to the transformation properties of the momentum operator and the adatom-interaction part of the Hamiltonian

$$\hat{\vec{p}} \to \hat{S}(t)\,\hat{\vec{p}}\,\hat{S}^{\dagger}(t) = \hat{\vec{p}}\,, \tag{2.7}$$

$$\hat{\mathcal{H}}_{\rm AI}(t) = \frac{\hat{\vec{p}}^{\,2}}{2m} + \frac{m}{2}\big(\hat{\vec{x}}-\hat{\vec{u}}(0)\big)\cdot\overleftrightarrow{\omega}^{2}\cdot\big(\hat{\vec{x}}-\hat{\vec{u}}(0)\big) - \hat{\vec{p}}\cdot\dot{\vec{u}}_d(t) \tag{2.8}$$

$$\stackrel{\rm DE}{\equiv} \frac{(\hat{\vec{p}}-m\dot{\vec{u}}_d(t))^2}{2m} + \frac{m}{2}\big(\hat{\vec{x}}-\hat{\vec{u}}(0)\big)\cdot\overleftrightarrow{\omega}^{2}\cdot\big(\hat{\vec{x}}-\hat{\vec{u}}(0)\big)\ . \tag{2.9}$$

Here $\dot{\vec{u}}_d(t) = \vec{v}_d(t)$ is the velocity of the movement of the bottom of the potential well and we used the dynamical equivalence between the two expressions of $\hat{\mathcal{H}}_{\rm AI}(t)$ since

they differ in a multiple of the unity operator only. This form of the transformed Hamiltonian may be found in [6], for example, where the dissipative properties of the film slipping over the vibrating substrate are considered.

Another, more common choice of the canonical transformation takes for $\hat{S}(t)$ the following expression

$$\hat{S}(t) = \exp\Big(\frac{i}{\hbar}\big(\hat{\vec{p}}\cdot\vec{u}_d(t) - m\hat{\vec{x}}\cdot\dot{\vec{u}}_d(t)\big)\Big)\ , \tag{2.10}$$

which may be rewritten in the form of Eq. (2.6), with the help of the Glauber identity. The momentum and the adatom-interaction part of the Hamitonian then transform as

$$\hat{\vec{p}} \to \hat{S}(t)\,\hat{\vec{p}}\,\hat{S}^{\dagger}(t) = \hat{\vec{p}} + m\dot{\vec{u}}_d(t)\ , \tag{2.11}$$

$$\hat{\mathcal{H}}_{\mathrm{AI}}(t) \overset{\mathrm{DE}}{\equiv} \frac{\hat{\vec{p}}^{\,2}}{2m} + \frac{m}{2}\big(\hat{\vec{x}} - \hat{\vec{u}}(0)\big)\cdot\overset{\leftrightarrow}{\omega}^{2}\cdot\big(\hat{\vec{x}} - \hat{\vec{u}}(0)\big) + m\ddot{\vec{u}}_d(t)\cdot\hat{\vec{x}}\ . \tag{2.12}$$

This form is easily interpreted in a physically transparent way. As already the transformation of the momentum suggests, this choice of the canonical transformation corresponds to the generalized Galilean transformation into the co-moving inertial frame of reference. Not only the coordinates, but also momenta are transformed in a correct way by this canonical transformation. As a consequence, we get the effective Hamiltonian in the form which fully corresponds to the description in the co-moving reference frame, including the inertial force $-m\ddot{\vec{u}}_d(t)$. This more physical approach is found more often in the literature, see [20, 19], for instance.

It should be noted, however, that all the canonically transformed problems are equivalent to the original one, regardless of the canonical transformation used. It is just a matter of taste which of them is chosen to make the problem easier to deal with. The translation of the transformed solution back into the original "reference frame" is rather straightforward. The equivalence of the transformed problems ensures that the dynamical evolution of, say, the mean value of the coordinate $\langle\hat{\vec{x}}\rangle(t)$ governed by the original Hamiltonian is the same as the dynamics of the transformed coordinate $\langle\hat{S}(t)\hat{\vec{x}}\hat{S}^{\dagger}(t)\rangle(t) = \langle\hat{\vec{x}}\rangle(t) + \vec{u}_d(t)$ or, in other words, that the dynamics of the coordinate in the transformed "reference frame" is the same as the dynamics of $\vec{x}(t) - \vec{u}_d(t)$ in the original one, which was exactly our requirement from the beginning. This feature will be explicitly illustrated in the next where we will calculate the effective equation of motion of the adatom above the vibrating substrate. These Galilean-transformation features together with the inertial effects will come out explicitly, illustrating thus in the particular case the general properties stemming from the canonical transformation reasoning. In the end, let us mention that a similar transformation may be done equally for the electronic degrees of freedom in the vibrating substrate as shown in [20], which again may help with the solution of the problems. We will not use these transformations in this work any more, even

though they would make some of the subsequent calculations slightly less complicated. However, we rather chose to take the direct approach and only recover the general transformation features in the final results.

## 2.2 Phenomenology

In this subsection, we will introduce the phenomenological derivation of the friction coefficient for the present model (called subsequently the *Persson's* model). It is clear that the phenomenological approach to a problem depends on the specific model since the solution stems from the physical insight into the particular physical mechanism responsible for the friction and, therefore, this approach does not suggest any general formal scheme to be employed in other cases. On the other hand, these heuristic arguments elucidate the true physical origin of the friction force in the particular case, which might be somewhat obscured by rather complicated formalism in the general scheme. That is why we believe that one example of this approach is helpful. Moreover, the phenomenological quantities evaluated at this level will subsequently enter as building blocks into more sophisticated formalism, as we will also see in the due course of the presentation of different theoretical methods.

To illuminate the physical mechanism responsible for the friction force in this model, which is the radiation of the adatom energy into the bulk via the emission of the phonons, we will at first calculate the lost radiation power of an oscillating point-like force into unbound elastic continuum. This would correspond to the friction force experienced by the adatom harmonically pinned inside the bulk continuum. Although from the point of view of a friction experiment this setup definitely does not make any sense, we use it to identify the object of the main interest for the evaluation of the friction – the *retarded Green's function of the phonon field*. In the second part we will, in the analogous manner, calculate the friction coefficient for the correct setup of the semi-infinite half-space.

### 2.2.1 Basic definitions and notation

Let us consider homogeneous, isotropic, linearly elastic continuum. The constitution relation between the strain tensor and the deformation tensor of the material is given by the generalized Hook's law $\tau_{ij} = C_{ijkl}e_{kl}$ (summation over repeated indexes is assumed everywhere), with the deformation tensor $e_{kl}$ given by $e_{ij} = \frac{1}{2}\left(\frac{\partial u_i}{\partial x_j} + \frac{\partial u_j}{\partial x_i}\right)$ and the elastic constants tensor

$$C_{ijkl} = \lambda\delta_{ij}\delta_{kl} + \mu(\delta_{ik}\delta_{jl} + \delta_{il}\delta_{jk}) \ , \tag{2.13}$$

$\lambda$ and $\mu$ being the Lamé constants. The strain tensor is then[2]

$$\tau_{ij} = \lambda\delta_{ij}e_{kk} + 2\mu e_{ij} \ , \tag{2.14}$$

and, inserting this relation into the general equation of motion of the continuum

$$\varrho\frac{\partial^2 u_i}{\partial t^2} = \frac{\partial \tau_{ij}}{\partial x_j} + F_i^{\rm ext} \ , \tag{2.15}$$

where $\vec{F}^{\rm ext}$ is volume density of an external force, we get

$$\varrho\frac{\partial^2 \vec{u}}{\partial t^2} = (\lambda+\mu)\nabla{\rm div}\vec{u} + \mu\triangle\vec{u} + \vec{F}^{\rm ext} \ . \tag{2.16}$$

The equation for the Green's function of the elastic movement of the continuum is given by

$$\left(\varrho\frac{\partial^2}{\partial t^2}\delta_{ij} - (\lambda+\mu)\frac{\partial}{\partial x_i}\frac{\partial}{\partial x_j} - \mu\frac{\partial^2}{\partial x_l\partial x_l}\delta_{ij}\right)G_{jk}(\vec{r},\vec{r}\,',t-t') = -\delta_{ik}\delta(t-t')\delta(\vec{r}-\vec{r}\,') \tag{2.17}$$

with the appropriate boundary conditions.

Introducing the direct and inverse temporal Fourier transform by the following relations

$$\begin{aligned} G_{ij}(\vec{r},\vec{r}\,',\omega) &= \int_{-\infty}^{\infty} dt\, G_{ij}(\vec{r},\vec{r}\,',t)\, e^{i\omega t} \ , \\ G_{ij}(\vec{r},\vec{r}\,',t) &= \int_{-\infty}^{\infty} \frac{d\omega}{2\pi}\, G_{ij}(\vec{r},\vec{r}\,',\omega)\, e^{-i\omega t} \ , \end{aligned} \tag{2.18}$$

the equation for the Green's function in the Fourier picture has the form

$$\left(\varrho\omega^2\delta_{ij} + (\lambda+\mu)\frac{\partial}{\partial x_i}\frac{\partial}{\partial x_j} + \mu\frac{\partial^2}{\partial x_l\partial x_l}\delta_{ij}\right)G_{jk}(\vec{r},\vec{r}\,',\omega) = \delta_{ik}\delta(\vec{r}-\vec{r}\,') \ . \tag{2.19}$$

As usually, we must specify the regularization method for the evaluation of the inverse Fourier transform since the singularities of the transformed Green's function may lie (and indeed lie) on the real axis in the complex $\omega$-plane, i. e. in the integration path of the inverse transform. This is accomplished by prescribing the path around poles. These prescriptions differ for different kinds of the Green's functions. To get the *causal* Green's function, it is necessary to substitute in the upper expression $\omega^2 \to \omega^2 + i\epsilon$, while for the *retarded* one $\omega^2 \to \omega^2 + i\epsilon\,{\rm sign}\omega$. It is known [21] that thus calculated Green's functions are identical to the corresponding quantum-mechanical Green's functions of the phonon field defined via T-product, commutators, etc. in the *harmonic case*, i. e. for the *free Green's functions* in terms of the perturbative quantum field theory.

[2]The elastic potential energy $U^{\rm el}_{\rm pot} = \frac{1}{2}\tau_{ij}e_{ij}$ expressed in terms of the derivatives of the phonon field enters the potential energy part of the substrate Hamiltonian (2.1a).

### 2.2.2 Radiation of point dipole into unbound elastic continuum

Let us now calculate the power lost by a point-like dipole (i. e. a point time-dependent external force) into the unbound continuum. The power produced by an external volume force is given by

$$P(t) = \int_{R^3} \vec{F}^{\text{ext}}(\vec{r},t) \cdot \frac{\partial \vec{u}(\vec{r},t)}{\partial t}\, d^3\vec{r}\,, \tag{2.20}$$

where $\vec{u}(\vec{r},t)$ is the solution of the equation of motion and is therefore given by the convolution of the retarded Green's function with the source term on the right hand side of the equation of motion (the external force). This is expressed by the following equation

$$u_i(\vec{r},t) = -\int_{-\infty}^{\infty} dt' \int_{R^3} d^3\vec{r}\,' \, G^R_{ij}(\vec{r}-\vec{r}\,', t-t')\, F^{\text{ext}}_j(\vec{r}\,', t')\ , \tag{2.21}$$

where $G^R(\vec{r}-\vec{r}\,',t) \equiv G^R(\vec{r},\vec{r}\,',t)$ means the retarded Green's function which is zero for $t<0$ and, thus, the integration over $t'$ actually runs only over the interval $(-\infty, t)$ . The resulting absorbed power is

$$P(t) = -\int_{R^3} d^3\vec{r} \int_{R^3} d^3\vec{r}\,' \int_{-\infty}^{t} dt'\, F^{\text{ext}}_i(\vec{r},t)\, \frac{\partial}{\partial t} G^R_{ij}(\vec{r}-\vec{r}\,', t-t')\, F^{\text{ext}}_j(\vec{r}\,', t')\ . \tag{2.22}$$

Note that in this case the Green's functions are functions of the difference $\vec{r}-\vec{r}\,'$ only, which allows us to define the spatial Fourier transform with respect to this difference as follows

$$\begin{aligned} G_{ij}(\vec{k},\bullet) &= \int_{R^3} d^3\vec{r}\, G_{ij}(\vec{r},\bullet)\, e^{-i\vec{k}\cdot\vec{r}}\ , \\ G_{ij}(\vec{r},\bullet) &= \int_{R^3} \frac{d^3\vec{k}}{(2\pi)^3}\, G_{ij}(\vec{k},\bullet)\, e^{i\vec{k}\cdot\vec{r}}\ . \end{aligned} \tag{2.23}$$

The bullet "$\bullet$" denotes the temporal variable, which may be either $t$ or $\omega$. The equation (2.19) then reads

$$\left(\varrho\omega^2\delta_{ij} - (\lambda+\mu)k_ik_j - \mu k^2\delta_{ij}\right) G_{jk}(\vec{k},\omega) = \delta_{ik}\ , \tag{2.24}$$

with the appropriate substitution for $\omega^2$. To resolve this equation, one has to invert the matrix standing before $G_{jk}$. It may be done easily by introducing the longitudinal and transverse projectors $\mathcal{P}^L_{ij} = \frac{k_ik_j}{k^2}$ and $\mathcal{P}^T_{ij} = \delta_{ij} - \mathcal{P}^L_{ij} = \delta_{ij} - \frac{k_ik_j}{k^2}$. Projectors are mutually orthogonal and therefore the inverse of a matrix $A_{ij} = A_L\mathcal{P}^L_{ij} + A_T\mathcal{P}^T_{ij}$

is simply given by $A_{ij}^{-1} = {A_L}^{-1}\mathcal{P}_{ij}^L + {A_T}^{-1}\mathcal{P}_{ij}^T$. Thus, for Green's function we obtain

$$G_{ij}(\vec{k},\omega) = \frac{\frac{k_i k_j}{k^2}}{\varrho(\omega^2 - c_L^2 k^2)} + \frac{\delta_{ij} - \frac{k_i k_j}{k^2}}{\varrho(\omega^2 - c_T^2 k^2)} \ , \tag{2.25}$$

where $c_L = \sqrt{\frac{\lambda+2\mu}{\varrho}}$ and $c_T = \sqrt{\frac{\mu}{\varrho}}$ are the velocities of the longitudinal and transverse sound waves in the bulk material, respectively.

Expressing the convolution involved in the above relation for the emitted power via the Fourier transform of Green's function and the force field, we obtain

$$P(t) = -\int_{R^3} d^3\vec{r}\, F_i^{\rm ext}(\vec{r},t)\, \frac{\partial}{\partial t} \int_{R^4} \frac{d^3\vec{k}d\omega}{(2\pi)^4}\, G_{ij}^R(\vec{k},\omega)\, F_j^{\rm ext}(\vec{k},\omega)\, e^{-i(\omega t - \vec{k}\cdot\vec{r})} \ . \tag{2.26}$$

Inserting into this equation the form of $\vec{F}^{\rm ext}(\vec{r},t) = \delta(\vec{r})\, \vec{f}^{\rm ext}(t)$ which corresponds to the point force, one gets

$$P(t) = -f_i^{\rm ext}(t)\, \frac{\partial}{\partial t} \int_{-\infty}^{\infty} \frac{d\omega}{2\pi}\, e^{-i\omega t}\, f_j^{\rm ext}(\omega) \int_{R^3} \frac{d^3\vec{k}}{(2\pi)^3}\, G_{ij}^R(\vec{k},\omega) \tag{2.27}$$

because thanks to the point-like form of the external force its spatial Fourier transform does not depend on $\vec{k}$. The Green's function is now given by the equation (2.25) with an appropriate prescription of avoiding its poles in performing the inverse transform. Let us calculate the expression $-\int_{R^3} \frac{d^3\vec{k}}{(2\pi)^3}\, G_{ij}^R(\vec{k},\omega)$. The projectors may be simply integrated over angular variables in $d^3\vec{k}$ and this integration yields

$$\begin{aligned} \int_{4\pi} \frac{d\Omega_{\vec{k}}}{4\pi} \mathcal{P}_{ij}^L &= \frac{1}{3}\,\delta_{ij} \ , \\ \int_{4\pi} \frac{d\Omega_{\vec{k}}}{4\pi} \mathcal{P}_{ij}^T &= \frac{2}{3}\,\delta_{ij} \ . \end{aligned} \tag{2.28}$$

It is therefore enough to evaluate the expression

$$\int_0^{\frac{1}{a}} \frac{k^2 dk}{2\pi^2\varrho}\, \frac{1}{v^2k^2 - \omega^2 - i\epsilon{\rm sign}\omega} \tag{2.29}$$

with $k = |\vec{k}| = \sqrt{\vec{k}\cdot\vec{k}}$, where we have introduced the physical cut-off in $k$ of the order of inverse lattice constant $a$ as the original integral obviously diverges. The computation of the above integral in the leading terms of $\frac{1}{a}$ (i. e. the terms of the order of $a$ and higher were set to zero) yields

$$\int_0^{\frac{1}{a}} \frac{k^2 dk}{2\pi^2\varrho}\, \frac{1}{v^2k^2 - \omega^2 - i\epsilon{\rm sign}\omega} = \frac{1}{2\pi^2\varrho\, v^2}\, \frac{1}{a} + \frac{i\omega}{4\pi\varrho\, v^3} \ . \tag{2.30}$$

Putting this result into the relation (2.27) for the radiation power and performing the inverse Fourier transform, we obtain

$$P(t) = \frac{1}{2\pi^2 \varrho}\,\frac{1}{c^2}\,\frac{1}{a}\,\vec{f}^{\,\mathrm{ext}}(t)\cdot\frac{d}{dt}\vec{f}^{\,\mathrm{ext}}(t) - \frac{1}{4\pi\varrho}\,\frac{1}{c^3}\,\vec{f}^{\,\mathrm{ext}}(t)\cdot\frac{d^2}{dt^2}\vec{f}^{\,\mathrm{ext}}(t)\ . \tag{2.31}$$

The factors $\frac{1}{c^n}$ in (2.31) are defined as averages of the sound velocities over the longitudinal and transverse modes by the following

$$\frac{1}{c^n} \equiv \frac{1}{3c_L^n} + \frac{2}{3c_T^n}\ . \tag{2.32}$$

The upper expression for the power may still be manipulated to a more convenient form

$$\begin{aligned} P(t) = {} & \frac{1}{4\pi^2 \varrho}\,\frac{1}{c^2}\,\frac{1}{a}\,\frac{d}{dt}\Big(\vec{f}^{\,\mathrm{ext}}(t)\cdot\vec{f}^{\,\mathrm{ext}}(t)\Big) - \frac{1}{4\pi\varrho}\,\frac{1}{c^3}\,\frac{d}{dt}\Big(\vec{f}^{\,\mathrm{ext}}(t)\cdot\frac{d}{dt}\vec{f}^{\,\mathrm{ext}}(t)\Big) \\ & + \frac{1}{4\pi\varrho}\,\frac{1}{c^3}\,\frac{d}{dt}\vec{f}^{\,\mathrm{ext}}(t)\cdot\frac{d}{dt}\vec{f}^{\,\mathrm{ext}}(t)\ . \end{aligned} \tag{2.33}$$

The first two terms in this result are of the form of the total time derivative and thus cannot represent radiative contribution to the lost power. On the other hand, the third term is exactly what we searched for. This term is not potential (i. e. of the form of the total time derivative) and is always non-negative. That is why we will identify this term with the radiative power produced by the point dipole in the continuum. Moreover, this term is finite and does not depend on the cut-off. Thus, we come to the final result of this section giving the radiative power produced by the point dipole as[3]

$$P^{\mathrm{rad}}(t) = \frac{1}{4\pi\varrho}\,\frac{1}{c^3}\left(\frac{d\vec{f}^{\,\mathrm{ext}}(t)}{dt}\right)^2\ . \tag{2.34}$$

We will now apply this result to the calculation of the phononic contribution to the sliding friction of the motion of an adparticle. Let us assume that the adatom-phonon interaction is given by an analogous term to the one in the Persson's Hamiltonian, namely,

$$H_{\mathrm{int}} = \frac{m\omega_0^2}{2}\big(\vec{x}(t) - \vec{u}(0,t)\big)^2\ . \tag{2.35}$$

Here $\vec{x}(t)$ is considered to be a prescribed trajectory of the adatom motion. On the elastic continuum then an external point force acts which is given by

$$\vec{F}^{\,\mathrm{ext}}(\vec{r},t) = \delta(\vec{r})\, m\omega_0^2\vec{x}(t)\ . \tag{2.36}$$

[3]This formula is an exact analogy to the power emitted by the Hertz dipole in the classical electrodynamics.

The power radiated into the bulk by the motion of the adparticle is therefore

$$P^{\mathrm{rad}}(t) = \frac{m^2\omega_0^4}{4\pi\varrho}\,\frac{1}{c^3}\,\dot{\vec{x}}(t)^2 \ . \tag{2.37}$$

Assuming that the interaction of the adatom with the quantized phononic field causes that a friction force linear in the adatom velocity $\vec{F}_{\mathrm{friction}}(t) = -m\gamma^{\mathrm{ph}}\dot{\vec{x}}(t)$ appears, we may set the power lost by the action of such a force equal to the calculated power lost by the emission of the phonons. The energy of the adparticle lost per time unit is

$$\frac{dE^{\mathrm{adp}}(t)}{dt} = -m\gamma^{\mathrm{ph}}\dot{\vec{x}}(t)^2 = -P^{\mathrm{rad}}(t) \tag{2.38}$$

and equals in the absolute value to the radiative power absorbed by the elastic continuum. We see that the assumption on the character of the emerged friction force (linearity in velocity) is consistent with our results and get for the phononic contribution to the sliding friction coefficient $\gamma^{\mathrm{ph}}$ the expression

$$\gamma^{\mathrm{ph}} = \frac{m\omega_0^4}{4\pi\varrho}\,\frac{1}{c^3} \ . \tag{2.39}$$

### 2.2.3 The Green's function for a halfspace

Now, we are going to deal with a more adequate model for the description of the damping of adsorbates. Our present model consists of a semi-infinite elastic continuum with a flat plane boundary on which the adsorbate resides. Let us formulate the problem. We have again the continuum considered in the previous sections, but now it extends only in the halfspace $z \leq 0$. In this case, we must also specify the boundary conditions on the surface. Assuming the surface to be free, we set the boundary condition to zero force on the surface. In fact, on the surface there is the adatom which acts by a surface force on the continuum, but we will consider this source term to be the volume force term being placed just under the surface and then take the limit of its position approaching the surface from beneath. Both these methods give the same results (this statement is proven in [22], Section 5.6). The force acting on an elementary surface with the normal $\vec{\nu}$ in the continuum and/or on the surface is $\vec{F}_{\vec{\nu}}(\vec{r},t) = \overleftrightarrow{\tau}(\vec{r},t)\cdot\vec{\nu}$. Thus, our boundary condition on the surface plane $z = 0$ is $\tau_{i3}(\vec{r} = (x,y,0),t) = 0$ for all $i, x, y$ and $t$. In terms of the Green's

function components, the boundary condition reads

$$\left.\frac{\partial G_{1j}}{\partial z}\right|_{z=0} = -\left.\frac{\partial G_{3j}}{\partial x}\right|_{z=0}, \tag{2.40a}$$

$$\left.\frac{\partial G_{2j}}{\partial z}\right|_{z=0} = -\left.\frac{\partial G_{3j}}{\partial y}\right|_{z=0}, \tag{2.40b}$$

$$(\lambda+2\mu)\left.\frac{\partial G_{3j}}{\partial z}\right|_{z=0} = -\lambda\left.\left(\frac{\partial G_{1j}}{\partial x}+\frac{\partial G_{2j}}{\partial y}\right)\right|_{z=0}. \tag{2.40c}$$

The Green's function still satisfies the equation (2.19), but now it is not so easy to solve the equation since the translational invariance necessary for performing the spatial Fourier transform is broken in the $z$-direction. We may, of course, still perform the 2-dimensional Fourier transform in the $x, y$ variables, but this is not enough for reducing the defining equation for the Green's function into a simple algebraic matrix inverse like in the preceding case. Rather, the equation obtained after performing the Fourier transforms in the 2-dimensional spatial and the time domain is quite complicated matrix equation involving the first and second derivatives with respect to $z$. To transform this matrix relation into the most convenient form, we have to consider the general tensor structure of the Green's function first.

The Green's function is a function of the arguments $\vec{r}_{\|} - \vec{r}_{\|}\,', z, z'$, and $t$. After applying the Fourier transforms

$$G_{ij}(\vec{\kappa}, z, z', \omega) = \int_{R^3} d^2\vec{r}_{\|}dt\, G_{ij}(\vec{r}_{\|}, z, z', t)\, e^{i(\omega t - \vec{\kappa}\cdot\vec{r}_{\|})} \tag{2.41}$$

mentioned above, the Green's function is a function of $\vec{\kappa}, z, z'$, and $\omega$. The symbol $\vec{r}_{\|}$ means the 2-dimensional position vector in the $xy$ plane parallel with the surface. From geometrical reasoning it follows that all the components of the Green's function indexed by 1,2 (or $x, y$, respectively) behave like a 2-dimensional vector when one rotates the argument $\vec{r}_{\|}$ of the Green's function in the $xy$ plane, while all the components with the index 3 are scalars with respect to this transformation. To

illustrate this fact, let us write these transforming relations

$$\begin{aligned}
G_{11}(x,y) &= \sin^2\varphi\, G_{11}(0,r) - \sin\varphi\cos\varphi\, G_{12}(0,r) \\
&\quad - \sin\varphi\cos\varphi\, G_{21}(0,r) + \cos^2\varphi\, G_{22}(0,r)\ , \\
G_{12}(x,y) &= \sin\varphi\cos\varphi\, G_{11}(0,r) + \sin^2\varphi\, G_{12}(0,r) \\
&\quad - \cos^2\varphi\, G_{21}(0,r) - \sin\varphi\cos\varphi\, G_{22}(0,r)\ , \\
G_{13}(x,y) &= \sin\varphi\, G_{13}(0,r) + \cos\varphi\, G_{23}(0,r)\ , \\
G_{21}(x,y) &= \sin\varphi\cos\varphi\, G_{11}(0,r) - \cos^2\varphi\, G_{12}(0,r) \\
&\quad + \sin^2\varphi\, G_{21}(0,r) - \sin\varphi\cos\varphi\, G_{22}(0,r)\ , \\
G_{22}(x,y) &= \cos^2\varphi\, G_{11}(0,r) + \sin\varphi\cos\varphi\, G_{12}(0,r) \\
&\quad + \sin\varphi\cos\varphi\, G_{21}(0,r) + \sin^2\varphi\, G_{22}(0,r)\ , \\
G_{23}(x,y) &= -\cos\varphi\, G_{13}(0,r) + \sin\varphi\, G_{23}(0,r)\ , \\
G_{31}(x,y) &= \sin\varphi\, G_{31}(0,r) + \cos\varphi\, G_{32}(0,r)\ , \\
G_{32}(x,y) &= -\cos\varphi\, G_{31}(0,r) + \sin\varphi\, G_{32}(0,r)\ , \\
G_{33}(x,y) &= G_{33}(0,r)\ ,
\end{aligned} \tag{2.42}$$

where $x = r\cos\varphi$ and $y = r\sin\varphi$.

Thanks to the orthogonality of the rotation matrix appearing in the transformation relation between the original and rotated coordinates, exactly the same transformation relations hold also for the Green's function in the Fourier picture, more exactly when $x, y$ are replaced by $\kappa_x, \kappa_y$. This fact is crucial for the desired simplification of the equation for the Fourier-transformed Green's function. We can calculate the Green's function in specific points of the $\vec{\kappa}$-plane and then obtain all values by using the above relations. Such particularly convenient points are the points at the positive semiaxis $\vec{\kappa} = (0,\kappa) = (0,\kappa_y > 0)$, as we have already presumed in the upper relations. At these points, the equation for the Green's function in the Fourier picture reads

$$\mathcal{A}_{ij}\, G^R_{jk}(z;z',\kappa,\omega) = \delta_{ik}\,\delta(z-z') \tag{2.43}$$

with the matrix differential operator $\mathcal{A}_{ij}$ having the form

$$\mathcal{A} = \begin{pmatrix} \mu\left(\frac{d^2}{dz^2} + q_T^2\right) & 0 & 0 \\ 0 & \mu\frac{d^2}{dz^2} + \Gamma q_L^2 & i\kappa(\Gamma-\mu)\frac{d}{dz} \\ 0 & i\kappa(\Gamma-\mu)\frac{d}{dz} & \Gamma\frac{d^2}{dz^2} + \mu q_T^2 \end{pmatrix}\ , \tag{2.44}$$

where $\Gamma = \lambda + 2\mu$, $q_T^2 = \frac{\omega^2}{c_T^2} - \kappa^2 + i\epsilon\,\mathrm{sign}\omega$, and $q_L^2 = \frac{\omega^2}{c_L^2} - \kappa^2 + i\epsilon\,\mathrm{sign}\omega$. We see that the matrix differential operator has the block structure and therefore we expect the Green's function, which is its inverse, to have the same block structure. However, this must be allowed by the boundary conditions that must be consistent

with such a block structure. This is true in our case since the boundary condition (2.40) rewritten in the Fourier picture yields

$$\left.\frac{dG_{1j}(z;z',\kappa,\omega)}{dz}\right|_{z=0} = 0 \ , \tag{2.45a}$$

$$\left.\frac{dG_{2j}(z;z',\kappa,\omega)}{dz}\right|_{z=0} = -i\kappa\, G_{3j}(0;z',\kappa,\omega) \ , \tag{2.45b}$$

$$(\lambda+2\mu)\left.\frac{dG_{3j}(z;z',\kappa,\omega)}{dz}\right|_{z=0} = -i\kappa\lambda\, G_{2j}(0;z',\kappa,\omega) \ , \tag{2.45c}$$

and, thus, we have in fact two separate problems to find the Green's function. One is a 1-dimensional (i. e. scalar) differential equation for $G_{11}$ and the other a 2-dimensional (matrix) differential equation for the matrix consisting of $G_{22}, G_{23}, G_{32}$, and $G_{33}$. All other components are identically zero.

Tedious but straightforward calculations summarized in Appendix A yield

$$G^R_{11}(z;z') = \frac{\operatorname{sign}\omega}{2i\,\mu q_T}\left(e^{iq_T\operatorname{sign}\omega|z-z'|} + e^{-iq_T\operatorname{sign}\omega(z+z')}\right) \tag{2.46a}$$

and

$$\begin{aligned}
\begin{pmatrix} G^R_{22} & G^R_{23} \\ G^R_{32} & G^R_{33} \end{pmatrix}(z;z') = \\
\frac{1}{2i\varrho\omega^2}\Bigg\{ & e^{iq_L\operatorname{sign}\omega|z-z'|}\begin{pmatrix} \frac{\kappa^2}{q_L}\operatorname{sign}\omega & \kappa\operatorname{sign}(z-z') \\ \kappa\operatorname{sign}(z-z') & q_L\operatorname{sign}\omega \end{pmatrix} \\
& + e^{iq_T\operatorname{sign}\omega|z-z'|}\begin{pmatrix} q_T\operatorname{sign}\omega & -\kappa\operatorname{sign}(z-z') \\ -\kappa\operatorname{sign}(z-z') & \frac{\kappa^2}{q_T}\operatorname{sign}\omega \end{pmatrix} \\
& + e^{-iq_L\operatorname{sign}\omega(z+z')}\frac{\left(\frac{q_T^2}{\kappa^2}-1\right)^2 - 4\frac{q_Lq_T}{\kappa^2}}{\left(\frac{q_T^2}{\kappa^2}-1\right)^2 + 4\frac{q_Lq_T}{\kappa^2}}\begin{pmatrix} -\frac{\kappa^2}{q_L}\operatorname{sign}\omega & -\kappa \\ \kappa & q_L\operatorname{sign}\omega \end{pmatrix} \\
& + e^{-iq_T\operatorname{sign}\omega(z+z')}\frac{\left(\frac{q_T^2}{\kappa^2}-1\right)^2 - 4\frac{q_Lq_T}{\kappa^2}}{\left(\frac{q_T^2}{\kappa^2}-1\right)^2 + 4\frac{q_Lq_T}{\kappa^2}}\begin{pmatrix} q_T\operatorname{sign}\omega & -\kappa \\ \kappa & -\frac{\kappa^2}{q_T}\operatorname{sign}\omega \end{pmatrix} \\
& + e^{-i\operatorname{sign}\omega(q_Lz+q_Tz')}\,4\frac{\frac{q_T^2}{\kappa^2}-1}{\left(\frac{q_T^2}{\kappa^2}-1\right)^2 + 4\frac{q_Lq_T}{\kappa^2}}\begin{pmatrix} q_T\operatorname{sign}\omega & -\kappa \\ -\frac{q_Lq_T}{\kappa} & q_L\operatorname{sign}\omega \end{pmatrix} \\
& + e^{-i\operatorname{sign}\omega(q_Tz+q_Lz')}\,4\frac{\frac{q_T^2}{\kappa^2}-1}{\left(\frac{q_T^2}{\kappa^2}-1\right)^2 + 4\frac{q_Lq_T}{\kappa^2}}\begin{pmatrix} q_T\operatorname{sign}\omega & \frac{q_Lq_T}{\kappa} \\ \kappa & q_L\operatorname{sign}\omega \end{pmatrix}\Bigg\}
\end{aligned} \tag{2.46b}$$

for all $z, z' \le 0$ and $\vec{\kappa} = (0, \kappa > 0)$ assumed everywhere.

### 2.2.4 Radiation of point surface dipole into halfspace

Let us now employ the results obtained in the previous section to calculate the power lost by radiation of a point dipole lying on the surface of the semi-infinite continuum. To do so, we use an analogy of the relation (2.27) for our present case. Since the surface is now present, we are interested in the quantity

$$\lim_{z\to 0^-, z'\to 0^-} \int_{R^2} \frac{d^2\vec{\kappa}}{(2\pi)^2}\, G^R_{ij}(\vec{\kappa}, z, z', \omega) \ ,$$

where $G^R_{ij}(\vec{\kappa}, z, z', \omega)$ denotes the Green's function for the halfspace in a general point of the $\vec{\kappa}$-plane. We must use the analogy of the relations (2.42) to express that quantity by means of the values at special points stated above. The limit cannot be put into the integrand thanks to the off-diagonal terms containing $\mathrm{sign}(z-z')$, but when we first integrate over the angle variable $\varphi$ in $d^2\vec{\kappa}$, the off-diagonal terms vanish and the limit makes no problems. Let us denote by $\langle G^R_{ij}(\kappa, z, z', \omega)\rangle$ the quantity $\int_0^{2\pi} \frac{d\varphi}{2\pi}\, G^R_{ij}(\kappa, \varphi, z, z', \omega)$, i. e. the components of the Green's function averaged over the direction of $\vec{\kappa}$. Since $G^R_{ij}(\kappa, \varphi, z, z', \omega)$ satisfy (2.42), we easily see that

$$\begin{aligned} \langle G^R_{11}(\kappa)\rangle = \langle G^R_{22}(\kappa)\rangle &= \frac{1}{2}\big(G^R_{11}(0,\kappa) + G^R_{22}(0,\kappa)\big) \ , \\ \langle G^R_{33}(\kappa)\rangle &= G^R_{33}(0,\kappa) \ . \end{aligned} \tag{2.47}$$

All other components of the averaged Green's function are zero. Taking the limit is trivial now and we finally get

$$\begin{aligned} \langle G^R_{11}(\kappa, z=0, z'=0, \omega)\rangle = \langle G^R_{22}\rangle &= \frac{\mathrm{sign}\omega}{2i}\left(\frac{1}{\mu q_T} + \frac{q_T}{\varrho\omega^2}\frac{\left(\frac{q_T^2}{\kappa^2}+1\right)^2}{\left(\frac{q_T^2}{\kappa^2}-1\right)^2 + 4\frac{q_L q_T}{\kappa^2}}\right) \ , \\ \langle G^R_{33}(\kappa, z=0, z'=0, \omega)\rangle &= \frac{\mathrm{sign}\omega\, q_L}{i\,\varrho\omega^2}\frac{\left(\frac{q_T^2}{\kappa^2}+1\right)^2}{\left(\frac{q_T^2}{\kappa^2}-1\right)^2 + 4\frac{q_L q_T}{\kappa^2}} \ . \end{aligned} \tag{2.48}$$

To obtain the final expression to be put into (2.27), we still have to integrate $\langle G^R_{ij}\rangle$ over $\kappa$. We are searching for the quantities $\int_0^{\frac{1}{a}} \frac{d\kappa\,\kappa}{2\pi}\langle G^R_{ij}(\kappa, z=0, z'=0, \omega)\rangle$. Using $\mu = \varrho c_T^2$ and changing the integration variable from $\kappa$ to $x = \frac{c_T^2\kappa^2}{\omega^2}$, we get

$$\begin{aligned} \int_0^{\frac{1}{a}} \frac{d\kappa\,\kappa}{2\pi}\langle G^R_{11}(\kappa)\rangle &= \frac{\omega}{8\pi i\,\varrho\, c_T^3}\int_0^{\frac{c_T^2}{a^2\omega^2}} dx\left(\frac{1}{\sqrt{1-x}} + \frac{\sqrt{1-x}}{(1-2x)^2 + 4x\sqrt{1-x}\,\sqrt{\left(\frac{c_T}{c_L}\right)^2 - x}}\right) \ , \\ \int_0^{\frac{1}{a}} \frac{d\kappa\,\kappa}{2\pi}\langle G^R_{33}(\kappa)\rangle &= \frac{\omega}{8\pi i\,\varrho\, c_T^3}\int_0^{\frac{c_T^2}{a^2\omega^2}} dx \frac{2\sqrt{\left(\frac{c_T}{c_L}\right)^2 - x}}{(1-2x)^2 + 4x\sqrt{1-x}\,\sqrt{\left(\frac{c_T}{c_L}\right)^2 - x}} \ . \end{aligned} \tag{2.49}$$

The value of the integral for $\langle G^R_{22}\rangle$ is the same as that for $\langle G^R_{11}\rangle$. Everywhere in the integrand there should be understood that $x \to x - i\epsilon\,\mathrm{sign}\omega$. More detailed analysis of the integrals yields the following results. The values of these integrals are generally complex numbers dependent on the upper integration limit and thus still dependent on $\omega$. Their real parts, however, do not depend on the upper limit for $a$ small enough. The imaginary part depends on the upper limit as $\frac{c_T}{a\omega}$ for small $a$. This is an exact analogy with the case of the unbound continuum. We may therefore easily identify the terms corresponding to the radiative power exactly like in the previous case. The only difference here is that the result is not totally isotropic thanks to the presence of the surface, but there are two different terms. The first one is isotropic in the $xy$ plane and the other corresponds to the $z$ component (i. e. perpendicular to the surface) of the driving force. The result analogous to the equation (2.34) of the unbound case now reads

$$P^{\mathrm{rad}}(t) = \frac{1}{8\pi\,\varrho\,c_T^3}\left(\xi_{\|}\left(\,\dot{f}_x^{\mathrm{ext}}(t)^2 + \dot{f}_y^{\mathrm{ext}}(t)^2\,\right) + \xi_{\perp}\,\dot{f}_z^{\mathrm{ext}}(t)^2\right)\ , \tag{2.50}$$

where

$$\begin{aligned}
\xi_{\|} &= \mathrm{Re}\int_0^\infty dx\left(\frac{1}{\sqrt{1-x}} + \frac{\sqrt{1-x}}{(1-2x)^2 + 4x\sqrt{1-x}\,\sqrt{\left(\frac{c_T}{c_L}\right)^2 - x}}\right)\ , \\
\xi_{\perp} &= \mathrm{Re}\int_0^\infty dx\,\frac{2\sqrt{\left(\frac{c_T}{c_L}\right)^2 - x}}{(1-2x)^2 + 4x\sqrt{1-x}\,\sqrt{\left(\frac{c_T}{c_L}\right)^2 - x}}\ .
\end{aligned} \tag{2.51}$$

Using our interaction Hamiltonian of an adparticle adsorbed on the surface with two harmonic interaction constants giving rise to two different frequencies $\omega_{\|}$, $\omega_{\perp}$ corresponding to the motions parallel and perpendicular to the surface, respectively, instead of only one adsorbate frequency $\omega_0$, we may express the phononic contribution to the sliding friction coefficients of the parallel and perpendicular motion of the adsorbate particle as follows

$$\begin{aligned}
\gamma_{\|}^{\mathrm{ph}} &= \frac{m}{8\pi\varrho}\left(\frac{\omega_{\|}}{c_T}\right)^3 \omega_{\|}\,\xi_{\|}\ , \\
\gamma_{\perp}^{\mathrm{ph}} &= \frac{m}{8\pi\varrho}\left(\frac{\omega_{\perp}}{c_T}\right)^3 \omega_{\perp}\,\xi_{\perp}\ .
\end{aligned} \tag{2.52}$$

These results are the same as those by B. N. J. Persson [17]. Let us now briefly comment on the method of evaluation of the integrals for the $\xi$'s. Seemingly, the real parts of the integrands are only nonzero for integration interval $(0, 1)$. For higher $x$'s the arguments appear to be purely imaginary. This is, however, not true as we must always remember that $x$ in the integrand is regularized by the substitution

$x \to x - i\,\epsilon\,\mathrm{sign}\omega$. This is not essential in the region $x \in (0,1)$, but is necessary to consider in the range $x > 1$ since in this range the real parts of the denominators in the integrands may become zero. If this is the case, the regularization prescription yields a delta-peak contribution to the integrand. The position of this delta-peak corresponds to the root of the complicated denominator.

These considerations may physically be explained neatly. The continuous distribution in the range $x \in (0,1)$ is due to the emission of bulk phonons whose projections of the wavevector onto the surface plane $\vec{\kappa}$ are allowed in the range $(0, \frac{\omega}{c_L})$ for longitudinal phonons and $(0, \frac{\omega}{c_T})$ for transverse ones (for a given $\omega$). As $c_L > c_T$, these intervals transfer onto the $x$-axis as $(0, \left(\frac{c_T}{c_L}\right)^2 < 1)$ and $(0,1)$. No values of $\kappa > \frac{\omega}{c_T}$ (i. e. $x > 1$) are allowed for the bulk phonons. However, in the situation of the continuum with surface there exists yet another vibrational mode. This mode is given by surface phonons localized along the surface. The velocity of this mode is smaller than the bulk ones and therefore for a given $\omega$ its wavevectors are longer then any bulk projections (i. e. $x_{\mathrm{surf}} > 1$). Moreover, since this mode is constrained onto the surface plane, the dispersion relation is also 2-dimensional and this mode appears as delta function peak (corresponding to a unique dispersion relation) in the surface projected density of phononic states that we are using in these calculations. The condition that the denominator equals zero is the same one as the dispersion relation condition for *surface Rayleigh waves* in [22], Section 3.4. If $x_{\mathrm{surf}} > 1$ is the root of the denominator, the dispersion relation for the Rayleigh waves is $\omega = \frac{c_T}{\sqrt{x_{\mathrm{surf}}}}\,|\vec{\kappa}|$. The phase velocity of this mode is thus $c_{\mathrm{surf}} = \frac{c_T}{\sqrt{x_{\mathrm{surf}}}} < c_T$.

## 2.3 Projection technique – perturbation theory

Let us now explore the behaviour of an adatom interacting with a reservoir represented by the phonon field in more detail than in the previous section. We will use the method of obtaining the *master equation* for the adatom's motion. In doing so, we will project out of the Liouville equation for the density matrix of the complete system (adatom plus reservoir) the degrees of freedom of the reservoir. We will formulate the problem as generally as possible first and put our specific model Hamiltonian into the obtained formulas after that.

### 2.3.1 General formalism

First, we set up the notation used in the following. Thus, let us assume that we have two systems labeled by A (adatom) and R (reservoir). Their Hamiltonians are $\hat{H}_A(t)$ and $\hat{H}_R$, respectively, and the interaction is $\hat{H}_{\mathrm{int}}(t)$. We assume that the part of the Hamiltonian corresponding to the reservoir is not time-dependent, but both the other parts may explicitly depend on time. It is convenient to employ

the *Dirac* or *interaction picture* in our considerations. In this quantum-mechanical picture all the operators are time-dependent and their evolution is governed by the unperturbed part of the Hamiltonian $\hat{H}_0(t) = \hat{H}_A(t) + \hat{H}_R$. The Liouville equation for the density matrix $\tilde{\rho}(t)$ of the composite system in the interaction representation reads

$$\frac{d\tilde{\rho}(t)}{dt} = \frac{1}{i\hbar}[\tilde{H}_{\rm int}(t), \tilde{\rho}(t)] = i\tilde{\mathcal{L}}_{\rm int}(t)\tilde{\rho}(t) \ . \tag{2.53}$$

From now on we will omit the hats over the quantum-mechanical operators, but keep the tilde over them to remind us of the fact that they must be expressed in the interaction picture. The calligraphic scripts will denote the superoperators acting in the vector space of ordinary quantum-mechanical operators. The $\tilde{\mathcal{L}}_{\rm int}(t)$ denotes the time-dependent interaction Liouville superoperator in the Dirac representation. Let us now follow the standard route of projection techniques (cf. [23] or [24]) to obtain the projected density matrix of the subsystem A only. If we have two complementary and mutually orthogonal superprojectors $\mathcal{P}$ and $\mathcal{Q}$ satisfying $\mathcal{P}^2 = \mathcal{P}, \mathcal{Q}^2 = \mathcal{Q}, \mathcal{P} + \mathcal{Q} = 1$, and $\mathcal{P}\cdot\mathcal{Q} = \mathcal{Q}\cdot\mathcal{P} = 0$, we may use the above Liouville equation to express formally only the projected part $\mathcal{P}\tilde{\rho}(t)$ of the full density matrix as

$$\begin{aligned} \frac{d\mathcal{P}\tilde{\rho}(t)}{dt} &= i\mathcal{P}\tilde{\mathcal{L}}_{\rm int}(t)\mathcal{P}\tilde{\rho}(t) + i\mathcal{P}\tilde{\mathcal{L}}_{\rm int}(t)\,\mathcal{Q}\tilde{\rho}(t) \ , \\ \frac{d\mathcal{Q}\tilde{\rho}(t)}{dt} &= i\mathcal{Q}\tilde{\mathcal{L}}_{\rm int}(t)\mathcal{P}\tilde{\rho}(t) + i\mathcal{Q}\tilde{\mathcal{L}}_{\rm int}(t)\mathcal{Q}\tilde{\rho}(t) \ . \end{aligned} \tag{2.54}$$

Expressing the quantity $\mathcal{Q}\tilde{\rho}(t)$ from the second equation and inserting it into the first, we get

$$\begin{aligned} \mathcal{Q}\tilde{\rho}(t) = {\rm Texp}\Big(i\int_{t_0}^{t} \mathcal{Q}\tilde{\mathcal{L}}_{\rm int}(\tau)\,d\tau\Big)\ \mathcal{Q}\tilde{\rho}(t_0) \\ + \int_{t_0}^{t} T{\rm exp}\Big(i\int_{\tau}^{t} \mathcal{Q}\tilde{\mathcal{L}}_{\rm int}(\xi)\,d\xi\Big)\, i\mathcal{Q}\tilde{\mathcal{L}}_{\rm int}(\tau)\,\mathcal{P}\tilde{\rho}(\tau)\,d\tau \end{aligned}$$

and

$$\begin{aligned} \frac{d\mathcal{P}\tilde{\rho}(t)}{dt} = i\mathcal{P}\tilde{\mathcal{L}}_{\rm int}(t)\mathcal{P}\tilde{\rho}(t) + i\mathcal{P}\tilde{\mathcal{L}}_{\rm int}(t)\,{\rm Texp}\Big(i\int_{t_0}^{t} \mathcal{Q}\tilde{\mathcal{L}}_{\rm int}(\tau)\,d\tau\Big)\ \mathcal{Q}\tilde{\rho}(t_0) \\ + i\mathcal{P}\tilde{\mathcal{L}}_{\rm int}(t)\int_{t_0}^{t} {\rm Texp}\Big(i\int_{\tau}^{t} \mathcal{Q}\tilde{\mathcal{L}}_{\rm int}(\xi)\,d\xi\Big)\, i\mathcal{Q}\tilde{\mathcal{L}}_{\rm int}(\tau)\,\mathcal{P}\tilde{\rho}(\tau)\,d\tau \ . \end{aligned} \tag{2.55}$$

Now we select the form of the projector $\mathcal{P}$. It will act on an arbitrary operator $\hat{f}$ in the Hilbert space of the adparticle and reservoir as

$$\mathcal{P}\hat{f} = \hat{\rho}_R^{\rm can} \otimes {\rm Tr}_R\,\hat{f} \ , \tag{2.56}$$

where $\hat{\rho}_R^{\rm can} = e^{-\beta \hat{H}_R}/Tr_R e^{-\beta \hat{H}_R}$ is the canonical density matrix of the reservoir and thus is an operator in the Hilbert space of the reservoir, while the partial trace is still an operator in the Hilbert space of the adatom. If the initial time density operator separates $\tilde{\rho}(t_0) \equiv \rho(t_0) = \rho_R^{\rm can} \otimes \rho_A(t_0)$ (we assume that the interaction and Schrődinger picture coincide at $t_0$), the second term in (2.55) vanishes. Furthermore, the first term may be simplified as follows

$$\begin{aligned} i\mathcal{P}\tilde{\mathcal{L}}_{\rm int}(t)\mathcal{P}\tilde{\rho}(t) &= i\rho_R^{\rm can}\,{\rm Tr}_R\big(\tilde{\mathcal{L}}_{\rm int}(t)\,\rho_R^{\rm can}\ {\rm Tr}_R\,\tilde{\rho}(t)\big) \\ &= \frac{1}{i\hbar}\,{\rm Tr}_R\big(\tilde{H}_{\rm int}(t)\rho_R^{\rm can}\big)\rho_R^{\rm can}\ {\rm Tr}_R\,\tilde{\rho}(t) - \frac{1}{i\hbar}\rho_R^{\rm can}\ {\rm Tr}_R\,\tilde{\rho}(t)\,{\rm Tr}_R\big(\rho_R^{\rm can}\tilde{H}_{\rm int}(t)\big) \\ &= i\tilde{\mathcal{L}}_{\rm int}^{\rm MF}(t)\mathcal{P}\tilde{\rho}(t)\ . \end{aligned} \tag{2.57}$$

The "mean-field" Liouvillian only acts in the adparticle subspace and is defined as

$$i\tilde{\mathcal{L}}_{\rm int}^{\rm MF}(t)\mathcal{P}\tilde{\rho}(t) = \frac{1}{i\hbar}\big[\tilde{H}_{\rm int}^{\rm MF}(t), \mathcal{P}\tilde{\rho}(t)\big] \tag{2.58a}$$

with

$$\tilde{H}_{\rm int}^{\rm MF}(t) = {\rm Tr}_R\big(\rho_R^{\rm can}\tilde{H}_{\rm int}(t)\big) = {\rm Tr}_R\big(\tilde{H}_{\rm int}(t)\rho_R^{\rm can}\big)\ . \tag{2.58b}$$

We may freely assume that $\tilde{H}_{\rm int}^{\rm MF}(t)$ equals zero since if it does not we can include it into $H_A(t)$ to get rid of this term. With this assumption and within the second order of the perturbation theory (Born approximation) in $H_{\rm int}(t)$, we obtain

$$\frac{d\mathcal{P}\tilde{\rho}(t)}{dt} = -\int_{t_0}^{t} d\tau \mathcal{P}\tilde{\mathcal{L}}_{\rm int}(t)\tilde{\mathcal{L}}_{\rm int}(\tau)\mathcal{P}\tilde{\rho}(\tau)\ . \tag{2.59}$$

Defining $\tilde{\sigma}(t) \equiv {\rm Tr}_R\,\tilde{\rho}(t)$, we get finally

$$\frac{d\tilde{\sigma}(t)}{dt} = -\frac{1}{\hbar^2}\int_{t_0}^{t} d\tau\,{\rm Tr}_R\Big(\big[\tilde{H}_{\rm int}(t), \big[\tilde{H}_{\rm int}(\tau), \rho_R^{\rm can}\tilde{\sigma}(\tau)\big]\big]\Big)\ . \tag{2.60}$$

### 2.3.2 Solution of the model

Now, we will utilize the above general expression for our model. First, we should check that the interaction term (2.1d) does not produce non-zero mean-field Hamiltonian as supposed above or we should add this mean-field term to the adatom part of the total Hamiltonian. The interaction part in the Dirac picture reads

$$\tilde{H}_{\rm int}(t) = \sum_{i=1}^{3}\Big(\frac{m\omega_{ii}^2}{2}\,\tilde{u}_i(0,t)^2 + m\omega_{ii}^2\,\big(u_i^d(t) - \tilde{x}_i(t)\big)\,\tilde{u}_i(0,t)\Big)\ , \tag{2.61}$$

with $\tilde{x}_i(t), \tilde{u}_i(0,t)$ being the coordinates operators of the adatom and phonons, respectively, in the Dirac picture. Their time dependence is given by the free evolution according to $\hat{H}_{\rm ads}(t)$ and $\hat{H}_{\rm sub}$, respectively. The interaction term proportional to $\tilde{u}_i(0,t)^2$ produces a non-zero mean-field interaction, however, this mean-field operator acts as a unity operator in the adatom subspace and, thus, may be omitted. Moreover, due to the averages over the canonical state of the reservoir in (2.60), the quadratic (in $\tilde{u}_i(0,t)$) interaction term does not mix with the linear one in (2.60) and, in addition, the contribution of the quadratic term used twice in (2.60) also vanishes. Therefore, we only need to consider the second (linear in $\tilde{u}_i(0,t)$) interaction term in that equation. If we put $\sum_{i=1}^{3} m\omega_{ii}^2 \left(u_i^d(t) - x_i\right) u_i(0)$ into (2.60), we obtain

$$\begin{aligned}\frac{d\tilde{\sigma}(t)}{dt} = -\frac{m^2}{\hbar^2}\sum_{i,j=1}^{3}\omega_{ii}^2\omega_{jj}^2\int_{t_0}^{t} d\tau \\ \Big[C_{ij}(t-\tau)\big(\tilde{x}_i(t)\tilde{x}_j(\tau)\tilde{\sigma}(\tau) - \tilde{x}_j(\tau)\tilde{\sigma}(\tau)\tilde{x}_i(t)\big) + \\ C_{ji}(\tau-t)\big(\hat{\sigma}(\tau)\tilde{x}_j(\tau)\tilde{x}_i(t) - \tilde{x}_i(t)\tilde{\sigma}(\tau)\tilde{x}_j(\tau)\big) + \\ \big(C_{ij}(t-\tau) - C_{ji}(\tau-t)\big)\big(\tilde{x}_i(t)\tilde{\sigma}(\tau) - \tilde{\sigma}(\tau)\tilde{x}_i(t)\big)u_j^d(0,\tau)\Big] ,\end{aligned} \tag{2.62}$$

where $C_{ij}(t) = \mathrm{Tr}_{\rm sub}\big(\rho_{\rm sub}^{\rm can}\,\tilde{u}_i(\vec{r}=0,t)\tilde{u}_j(\vec{r}\,'=0,0)\big)$ are the correlation functions of the phonon field. At this point we are ready to derive the equation of motion of the adparticle, more precisely, the equation of motion for the mean value of the adparticle's coordinate $\vec{x}(t) = \mathrm{Tr}_{\rm ads}\big(\tilde{\vec{x}}(t)\tilde{\sigma}(t)\big)$. We find

$$\begin{aligned}\dot{x}_i(t) &= \mathrm{Tr}_{\rm ads}\big(\dot{\tilde{x}}_i(t)\tilde{\sigma}(t)\big) + \mathrm{Tr}_{\rm ads}\big(\tilde{x}_i(t)\dot{\tilde{\sigma}}(t)\big) \\ &= \frac{p_i(t)}{m} ,\end{aligned} \tag{2.63}$$

$$\begin{aligned}\dot{p}_i(t) &= \mathrm{Tr}_{\rm ads}\big(\dot{\tilde{p}}_i(t)\tilde{\sigma}(t)\big) + \mathrm{Tr}_{\rm ads}\big(\tilde{p}_i(t)\dot{\tilde{\sigma}}(t)\big) \\ &= -m\omega_{ii}^2\big(x_i(t) - u_i^d(t)\big) - m^2\omega_{ii}^2\sum_{j=1}^{3}\omega_{jj}^2\int_{t_0}^{t} d\tau G_{ij}^R(0,0,t-\tau)\big(x_j(t) - u_j^d(t)\big) ,\end{aligned} \tag{2.64}$$

where dots denote time derivatives and the retarded Green's function

$$G_{ij}^R(\vec{r},\vec{r}\,',t) = \frac{1}{i\hbar}\big\langle\tilde{u}_i(\vec{r},t)\tilde{u}_j(\vec{r}\,',0) - \tilde{u}_j(\vec{r}\,',0)u_i(\vec{r},t)\big\rangle\theta(t) \tag{2.65}$$

of the phonon field has been introduced. The brackets denote the thermal average over the canonic state of the phonon field reservoir. In the above derivation, we used the equal-time commutation relations for $\tilde{x}_i(t)$ and $\tilde{p}_j(t)$.

Now, let us reformulate the above pair of equations into one equation for the mean value of position only. We introduce a new quantity $\vec{Q}(t) = \vec{x}(t) - \vec{u}^{\,d}(t)$ which has the meaning of the mean deviation of the oscillator coordinate from its potential minimum that moves together with $\vec{u}^{\,d}(t)$. Moreover, we will extend the time integration limits from $-\infty$ to $\infty$. The first limit means that we are interested in the stationary behaviour of the system only and, therefore, put the initial time point into infinite past so that all transients are over, the second limit has no effect as the Green's function is identically zero for $\tau > t$. Our final result reads

$$\ddot{Q}_i(t) + m\omega_{ii}^2 \sum_{j=1}^{3} \omega_{jj}^2 \int_{-\infty}^{\infty} d\tau G_{ij}^R(0,0,t-\tau) Q_j(\tau) + \omega_{ii}^2 Q_i(t) = -\ddot{u}_i^d(t) \ . \qquad (2.66)$$

If the driving is absent, we get the same equation for $x_i(t)$ with zero right hand side. Thus, we can see the physical meaning of the above result. In the presence of the driving force, the oscillator moves within its potential well whose position is changing due to the driven movement of the oscillator equilibrium position. The frequency and friction coefficient are the same as in the free (non-driven) case, but there is additionally the driving force due to the non-inertial effects that simply equals the inertial acceleration caused by the driven movement of the reference frame. This is the example of the Galilean transformation features promised at the beginning of the chapter.

The influence of the phononic reservoir on the adatom motion results in the term involving the retarded Green's function of the phonon field evaluated in $\vec{r} = 0$ and $\vec{r}\,' = 0$. We already encountered the same quantity in the phenomenological approach in Sec. 2.2.4. Namely, $G_{ij}^R(0,0,\omega)$ is evaluated in (2.49). A part of the discussion on the evaluation of these integrals concerning mainly their real parts is presented just after that equation. As for the imaginary parts, one should note that the integrals are divergent as $\sqrt{\Lambda}$, where $\Lambda$ is the upper integral limit. This leads to the following equation of motion for the adatom

$$\ddot{Q}_i(t) + \gamma_{ii}^{\mathrm{ph}} \dot{Q}_i(t) + \Big(\omega_{ii}^2 - \frac{m\omega_{ii}^4 Z_{ii}}{8\pi\varrho c_T^2 a}\Big) Q_i(t) = -\ddot{u}_i^d(t) \ , \qquad (2.67)$$

where the friction coefficients are given by (2.52) with (2.51) and the *renormalization constants* $Z_{ii}$ are

$$Z_{\parallel} = -\frac{a\omega}{c_T} \mathrm{Im} \int_0^{\frac{c_T^2}{a^2\omega^2}} dx \left( \frac{1}{\sqrt{1-x}} + \frac{\sqrt{1-x}}{(1-2x)^2 + 4x\sqrt{1-x}\,\sqrt{\left(\frac{c_T}{c_L}\right)^2 - x}} \right) \qquad (2.68)$$

$$Z_{\perp} = -\frac{a\omega}{c_T} \mathrm{Im} \int_0^{\frac{c_T^2}{a^2\omega^2}} dx \frac{2\sqrt{\left(\frac{c_T}{c_L}\right)^2 - x}}{(1-2x)^2 + 4x\sqrt{1-x}\,\sqrt{\left(\frac{c_T}{c_L}\right)^2 - x}} \ . \qquad (2.69)$$

Again, everywhere in the integrands there should be understood that $x \to x - i\epsilon\,\mathrm{sign}\omega$. We assume that the fraction $\frac{c_T}{a\omega}$ is large enough so that all the above integrals do not depend on it and $Z_{ii}$'s are constants with respect to $\omega$ and $a$. This assumption is equivalent to saying that the relevant adatom motion frequency represented by $\omega$ is small enough compared with the Debye frequency of the substrate assessed by $\frac{c_T}{a}$, which is indeed the condition of the applicability of the continuum description of the substrate. In the case of $\xi$'s, we already explicitly expressed this assumption by replacing the upper integration limit by infinity since the integrand has compact support (cf. (2.51)). Moreover, a closer inspection of the integrals involved shows that $Z_{ii}$'s are positive numbers dependent (in the limit specified above) on the ratio $\frac{c_T}{c_L}$ only, namely, $Z_{ii} \approx \frac{2}{1-(\frac{c_T}{c_L})^2}$.

One can see that the interaction with the reservoir causes the friction force exerted on the adatom as well as the change of the oscillator eigenfrequency. The eigenfrequency was *renormalized* by the interaction with the phonon field. The parameters $\omega_{ii}$ are to be fitted so as to yield correct values of the physical (renormalized) frequencies $\omega_{ii}^{r\,2} = \omega_{ii}^2 \left(1 - \frac{m\omega_{ii}^2 Z_{ii}}{8\pi\varrho c_T^2 a}\right)$. The above calculation is, however, perturbative and, therefore, valid only to the second order in the interaction term between the oscillator and the phonon field. Within this order of the perturbation theory, we should also replace the bare frequencies by the physical ones in all the physical quantities, namely, in the expression for $\gamma_{ii}^{\mathrm{ph}} = \frac{m\omega_{ii}^4}{8\pi\rho c_T^3}\xi_{ii}$. Within the second order of the perturbation theory, the quantity $\omega_{ii}$ in $\gamma_{ii}^{\mathrm{ph}}$ is simply replaced by $\omega_{ii}^r$ because the $\gamma_{ii}^{\mathrm{ph}}$ itself is already calculated in the second order. Therefore, our previous results are correct if the bare frequency is replaced by the renormalized one. The phenomenological approach used before only gave us the friction coefficients, while the renormalization of the eigenfrequencies is omitted in this approach. However, when the frequencies in the phenomenological result are considered to be the physical ones, this approach yields results correct even from the microscopic point of view.

## 2.4 Concluding remarks

We calculated the friction coefficient and the effective equation of motion of the adsorbate in a particular model which was an extension of the model considered originally by Persson and Rydberg [17] to the QCM experiment setup with the vibrating substrate. The phononic (or lattice) degrees of freedom were only considered in this model. On the other hand, the simple form of the interaction and the harmonic approximation used to describe the substrate phononic degrees of freedom enabled us to calculate exactly the relevant substrate response given by the retarded Green's function of the phonon field at the interaction site.

We illustrated two methods, namely, the phenomenological one stemming from the energy conservation argument and a simple perturbative projection technique. The phenomenological method clearly identifies the relevant mechanism causing friction — it is the irreversibility of the radiation of the adsorbate energy into the substrate mediated by the phonons outgoing into the bulk of the substrate which is responsible for the appearance of the irreversible friction force. The projection method which lies on the more rigorous grounds of the quantum mechanical approach only add to the results obtained by the phenomenology the renormalization of the bare adsorbate frequencies present in the effective equation of motion. The friction coefficients were obtained correctly already at the phenomenological level.

Both the methods used the retarded Green's function of the phonon field as the most relevant quantity. This quantity was calculated with the help of the surface Green's function method, namely, a tricky approach which employs an ansatz form of the Green's function satisfying the surface boundary conditions in terms of the Green's function in the unrestricted space. This shortcut method, although rather simple and straightforward, is not, to our knowledge, commonly known and no reference to it was found. It enables to solve the boundary condition problems in terms of the unrestricted solutions very efficiently and may be considered as a non-trivial technical contribution of this chapter. The knowledge of the retarded phononic Green's function itself could be useful also in other physical cases. Moreover, the identification of the retarded Green's function of the field interacting with the adsorbate as the relevant quantity yielding the friction coefficient is of general validity as will be exemplified in the next chapter concerning the electronic contribution to the friction force. The previous solutions of problems of this sort ([17, 18]) used the eigenmode expansion of the phonon fields, which method is not as general and powerful as the one using the Green's functions, although the final results obtained by the both are the same.

It would be in principle possible to use other theoretical methods mentioned in Introduction to solve this problem. In particular, due to the linear coupling of the phonon field and the harmonic approximation used for its description, it would possible to find the exact solution of the problem. However, the local coupling of the phonon field to the adsorbate (interaction term contains $\hat{\vec{u}}(\vec{r}=0)$) and the continuum description of the substrate makes the problem pathological (the $\delta$-function impurity in three dimensions is an unstable problem without the ground state) and one should consider a better specified discrete model. If the harmonic approximation and the linear coupling were preserved, the model would be still exactly soluble. However, the exact results would depend on the specific nature of the model considered and only the perturbative expansion of the exact results in the coupling strength is expected to reproduce the model-independent results obtained here (cf. [17]). Nevertheless, such discrete models should indeed be considered to describe realistic physical situations.

# Chapter 3

# Electronic friction force: adsorbates with dispersive interaction

## 3.1 Introduction to the electronic friction concept

In this chapter, we will discuss the part of the electronic contribution to the microscopic friction coefficient which is due to the dispersive interaction. This discussion will mainly have the form of review of the present results concerning the various aspects of the evaluation of the electronic part of the friction force. A unifying approach to plenty of methods currently employed will be used to give a general theoretical and conceptual framework to many of them. At the end, new results by the author concerning the problem of the electronic friction coefficient above a superconducting substrate are presented, and this problem, which is still open, is more thoroughly discussed.

First, let us briefly review the concept of the electronic friction. The bond of the adsorbates to the substrate is caused by the electronic degrees of freedom of both of them. According to the electronic nature of the bond, the two qualitative cases are usually distinguished, namely, the *chemisorption* and the *physisorption* cases. In the chemisorption cases, the coupling is basically of the chemical origin, i. e. the electronic charge distributions of the adsorbate and substrate are mixed, resulting in the chemical bond. Two subclasses are further considered encompassing the *covalent* and the *ionic* bond. From the point of view important for us, they differ mainly in the amount of the charge transfer between the adsorbate and substrate. In the ionic case, the adsorbate is partially charged and the bonding force is due to the Coulomb interaction of the charge with the substrate. In the covalent case, the adsorbate is not charged and the bonding interaction is of a purely quantum mechanical origin. This is a limit description since in all realistic cases both the

aspects are involved. Moreover, in all the cases (including the physisorption) the truly quantum-mechanical repulsive force caused by the overlapping of the electronic densities (the *Pauli repulsion*) is always present. In the physisorption case, the charge distributions of the adsorbate and substrate do not mix and the attractive force is only due to the quantum fluctuations of the electronic densities (the *van der Waals coupling*).

By the term dispersive interaction we mean the part of the interaction responsible for the attractive force between adsorbate and substrate, which is caused by the Coulomb interaction. This encompasses the cases of the van der Waals and ionic coupling. In the van der Waals coupling, the attractive force is caused by the Coulomb interaction of the quantum fluctuations of the charge densities of the adsorbate and substrate. In the cases which are classified as ionic the adsorbate is either partially charged or has a permanent dipole moment and these fixed classical charge distributions interact via the Coulomb field with the substrate electronic degrees of freedom. The problem of finding the friction force for these kinds of adsorbates means to find the generalization of the force to the nonstationary cases when the adsorbate moves with respect to the substrate. For a small velocity of the movement we expect that the attractive force remains the same while a dissipative force linear in the velocity appears. The evaluation of this force for the various physical setups as well as the justification of the above picture is the task of the theory of the electronic friction.

The case of the covalent bond is more complicated and will not be considered in our discussion. The bond in this case is of purely quantum-mechanical origin and the division of the interaction into the attractive part due to the Coulomb interaction and the Pauli repulsion is quite meaningless. Instead, the whole quantum mechanical bond is usually treated by the model description by the Anderson-Newns-like Hamiltonian and the evaluation of the friction force is done at this model level. This kind of solutions is rather different from the one used by us here and it constitutes another branch of the theoretical techniques. Moreover, our physical motivation is mainly by the physisorption cases. An overview of techniques used in various adsorption cases is given in [9]. Here, we will focus exclusively on the cases where the direct Coulomb attractive interaction plays a role.

The other part of the bonding interaction due to the Pauli repulsion is also expected to produce the dissipative component of the force in the non-stationary situation. However, this part of the electronic friction force is usually not considered. There is just one recent reference to the work by Sokoloff [13] in which the Pauli repulsion part of the friction force was modeled by the hard-sphere scattering of the substrate electrons from the hard core of the adsorbate atom. The additivity of the two contributions is a reasonable assumption in the physisorption case. Anyway, a better and more consistent description of the relation between the nature of the adsorption bond and the resulting friction force would be definitely helpful for the

more realistic calculations. This question has not been addressed yet properly and the answer to it would substantially improve the whole theory of the microscopic friction.

## 3.2 Linear response theory

Here, we present a simple generic model describing the interaction of an adatom with the substrate electronic degrees of freedom, using the Coulomb coupling. Namely, we use the following Hamiltonian

$$\hat{H}(t) = \hat{H}_{\rm ads} + \hat{H}_{\rm sub} + \hat{H}_{\rm int}(t) \ , \tag{3.1a}$$

where $\hat{H}_{\rm ads}$ denotes the Hamiltonian of the free dynamics of the adsorbate's charge distribution, while $\hat{H}_{\rm sub}$ corresponds to the free electronic dynamics of the substrate. $\hat{H}_{\rm int}(t)$ is interaction term reading

$$\hat{H}_{\rm int}(t) = \int d^3\vec{r} \int d^3\vec{r}\,' \, \hat{\rho}_{\rm ads}(\vec{r},t) V_C(\vec{r}-\vec{r}\,') \hat{\rho}_{\rm sub}(\vec{r}\,') \tag{3.1b}$$

with

$$\hat{\rho}_{\rm ads}(\vec{r},t) = \hat{\rho}_{\rm ads}(\vec{r}-\vec{r}_d(t)) \tag{3.1c}$$

being the explicitly time-dependent driven adsorbate charge distribution and

$$V_C(\vec{r}-\vec{r}\,') = \frac{1}{4\pi|\vec{r}-\vec{r}\,'|} \tag{3.1d}$$

the Coulomb potential. We may also use the above interaction Hamiltonian to express the operator of the force acting between the two charge distributions, i. e. the force exerted by the substrate on the adsorbate. This force operator is given by the electrostatics relation

$$\hat{\vec{F}}(t) = \int d^3\vec{r} \int d^3\vec{r}\,' \, \hat{\rho}_{\rm ads}(\vec{r},t) \big(-\nabla_{\vec{r}} V_C(\vec{r}-\vec{r}\,')\big) \hat{\rho}_{\rm sub}(\vec{r}\,') \ . \tag{3.2}$$

In the Dirac or interaction picture we get for the mean value of the force

$$\vec{F}(t) = \Big\langle \hat{\vec{F}}(t) \Big\rangle = \Big\langle \tilde{\rm T}\exp\Big(\frac{i}{\hbar}\int_{-\infty}^{t} d\tau \tilde{H}_{\rm int}(\tau)\Big) \, \tilde{\vec{F}}(t) \, {\rm Texp}\Big(-\frac{i}{\hbar}\int_{-\infty}^{t} d\tau \tilde{H}_{\rm int}(\tau)\Big) \Big\rangle \ , \tag{3.3}$$

which reduces in the first order of the perturbation theory in $\hat{H}_{\rm int}(t)$ to

$$\vec{F}(t) = \int_{-\infty}^{t} d\tau \frac{1}{i\hbar} \Big\langle \Big[ \tilde{\vec{F}}(t), \tilde{H}_{\rm int}(\tau) \Big] \Big\rangle \ . \tag{3.4}$$

This is an analog of the *Kubo formula* where the external driving is hidden in the $\tilde{H}_{\rm int}(\tau)$ term. In what follows, we will discuss this first order term in detail. Using it, we may derive with the help of various further approximation in the course of the derivation most of the so far published results. After that, we will also briefly comment on the higher order terms.

### 3.2.1 Adsorbates with classical charge distributions

First, let us assume that the charge distribution associated with the adsorbate is classical (corresponds to the ionic bond), which means that this distribution has no dynamics. This is formally expressed in our formalism by replacing the operator $\hat{\rho}_{\rm ads}(\vec{r},t)$ by the c-number function. The quantum-mechanical dynamics only remains in the substrate part of the Hamiltonian. Then the above linear response relation may be expanded as

$$\begin{aligned}\vec{F}(t) = \int_{-\infty}^{t} d\tau \int d^3\vec{r}\, d^3\vec{r}\,'\, d^3\vec{r}_1\, d^3\vec{r}_2\, \rho_{\rm ads}(\vec{r},t)\left(-\nabla_{\vec{r}} V_C(\vec{r}-\vec{r}_1)\right)\cdot \\ \frac{1}{i\hbar}\big\langle\big[\tilde{\rho}_{\rm sub}(\vec{r}_1,t),\tilde{\rho}_{\rm sub}(\vec{r}_2,\tau)\big]\big\rangle\, V_C(\vec{r}_2-\vec{r}\,')\,\rho_{\rm ads}(\vec{r}\,',\tau)\ .\end{aligned} \tag{3.5}$$

We see that the only quantum-mechanical object involved is the retarded Green's function of the substrate charge fluctuations. Namely, the evaluation of the retarded dielectric response function

$$\chi^R(\vec{r},\vec{r}\,';t-\tau) = \frac{1}{i\hbar}\big\langle\big[\tilde{\rho}_{\rm sub}(\vec{r},t),\tilde{\rho}_{\rm sub}(\vec{r}\,',\tau)\big]\big\rangle\theta(t-\tau) \tag{3.6}$$

plays the dominant role in the problem presently considered. The time dependence of the charge-density operators is given by the substrate part of the Hamiltonian exclusively and brackets $\langle\bullet\rangle$ denote the thermal average over the canonical state of the substrate electronic degrees of freedom. It is convenient to include the Coulomb interactions in (3.5) to the definition of the central object of our interest. Thus, we define the *Coulomb Green's function*

$$\begin{aligned}G_C^R(\vec{r},\vec{r}\,';t-\tau) &= \int d^3\vec{r}_1 \int d^3\vec{r}_2\, V_C(\vec{r}-\vec{r}_1)\,\chi^R(\vec{r}_1,\vec{r}_2;t-\tau)\,V_C(\vec{r}_2-\vec{r}\,') \\ &= \frac{1}{i\hbar}\big\langle\big[\tilde{\phi}_{\rm sub}(\vec{r},t),\tilde{\phi}_{\rm sub}(\vec{r}\,',\tau)\big]\big\rangle\theta(t-\tau)\ ,\end{aligned} \tag{3.7a}$$

where the Coulomb field operator $\tilde{\phi}_{\rm sub}(\vec{r},t)$ produced by the substrate charge distribution is given by

$$\tilde{\phi}_{\rm sub}(\vec{r},t) = \int d^3\vec{r}\,' V_C(\vec{r}-\vec{r}\,')\tilde{\rho}_{\rm sub}(\vec{r}\,',t)\ . \tag{3.7b}$$

This quantity may be regarded as the dressed part of the Green's function of the Coulomb field due to the interaction with the electronic degrees of freedom of the substrate. The bare Coulomb Green's function is just the Coulomb interaction potential (3.1d) (cf. [25], [26]). The Coulomb Green's function is crucial in most of electronic friction calculations and will be the subject of the subsequent discussions. However, we derive the microscopic friction coefficient of the electronic friction first, using the assumed knowledge of the Coulomb Green's function and Eq. (3.5). It can be rewritten in the form

$$\vec{F}(t) = \int_{-\infty}^{t} d\tau \int d^3\vec{r} \int d^3\vec{r}\,' \rho_{\rm ads}(\vec{r},t) \left(-\nabla_{\vec{r}}\, G_C^R(\vec{r},\vec{r}\,';t-\tau)\right) \rho_{\rm ads}(\vec{r}\,',\tau)\ . \tag{3.8}$$

Using (3.1c) and shift in integration variables, we come to the result

$$\vec{F}(t) = \int_{-\infty}^{t} d\tau \int d^3\vec{r} \int d^3\vec{r}\,' \rho_{\rm ads}(\vec{r}) \left(-\nabla_{\vec{r}}\, G_C^R(\vec{r}+\vec{r}_d(t),\vec{r}\,'+\vec{r}_d(\tau);t-\tau)\right) \rho_{\rm ads}(\vec{r}\,')\ , \tag{3.9}$$

which is the starting point for further manipulations. In order to find the linear friction coefficient, we expand the Green's function in the second spatial argument around the point $\vec{r}\,' + \vec{r}_d(t)$. That is, we make the expansion

$$\begin{aligned}
\vec{F}(t) &= \int_{-\infty}^{t} d\tau \int d^3\vec{r} \int d^3\vec{r}\,' \rho_{\rm ads}(\vec{r}) \\
&\qquad \left(-\nabla_{\vec{r}}\, G_C^R(\vec{r}+\vec{r}_d(t),\vec{r}\,'+\vec{r}_d(t)+(\vec{r}_d(\tau)-\vec{r}_d(t));t-\tau)\right) \rho_{\rm ads}(\vec{r}\,') \\
&= \int_{-\infty}^{t} d\tau \int d^3\vec{r} \int d^3\vec{r}\,' \rho_{\rm ads}(\vec{r}) \left(-\nabla_{\vec{r}}\, G_C^R(\vec{r}+\vec{r}_d(t),\vec{r}\,'+\vec{r}_d(t);t-\tau)\right) \rho_{\rm ads}(\vec{r}\,') \\
&+ \int_{-\infty}^{t} d\tau \int d^3\vec{r} \int d^3\vec{r}\,' \rho_{\rm ads}(\vec{r}) \left(\nabla_{\vec{r}}\,\nabla_{\vec{r}\,'}\, G_C^R(\vec{r}+\vec{r}_d(t),\vec{r}\,'+\vec{r}_d(t);t-\tau)\right) \\
&\qquad \rho_{\rm ads}(\vec{r}\,') \cdot \left(\vec{r}_d(t)-\vec{r}_d(\tau)\right) + \cdots
\end{aligned} \tag{3.10}$$

The first term in the expansion describes the immediate (static) force between the adsorbate and substrate. This is the usual *image-charge* attractive force on the charge above a dielectric surface. The force is explicitly time-dependent only through the immediate position of the adsorbate as

$$\begin{aligned}
\vec{F}_{\rm image}(\vec{r}_d(t)) &= \int_{-\infty}^{t} d\tau \int d^3\vec{r} \int d^3\vec{r}\,' \rho_{\rm ads}(\vec{r}) \\
&\qquad \left(-\nabla_{\vec{r}}\, G_C^R(\vec{r}+\vec{r}_d(t),\vec{r}\,'+\vec{r}_d(t);t-\tau)\right) \rho_{\rm ads}(\vec{r}\,') \\
&= \lim_{\omega\to 0} \int d^3\vec{r} \int d^3\vec{r}\,' \rho_{\rm ads}(\vec{r}) \left(-\nabla_{\vec{r}}\, G_C^R(\vec{r}+\vec{r}_d(t),\vec{r}\,'+\vec{r}_d(t);\omega)\right) \rho_{\rm ads}(\vec{r}\,')\ ,
\end{aligned} \tag{3.11}$$

where we have introduced the Fourier transform of the Coulomb Green's function

$$G_C^R(\vec{r},\vec{r}\,';\omega) = \int_{-\infty}^{\infty} dt\, G_C^R(\vec{r},\vec{r}\,';t)\, e^{i\omega t} \ . \tag{3.12}$$

The second order term in (3.10) corresponds to the friction force linear in velocity of the adsorbate. In this case, the force is a functional of the whole history of the movement of the adsorbate. By employing the following shortcut notation

$$\overleftrightarrow{\mathcal{G}}(\vec{r}_d(t);t-\tau) = \int d^3\vec{r} \int d^3\vec{r}\,' \rho_{\rm ads}(\vec{r}) \left(\nabla_{\vec{r}}\, \nabla_{\vec{r}\,'}\, G_C^R(\vec{r}+\vec{r}_d(t),\vec{r}\,'+\vec{r}_d(t);t-\tau)\right) \rho_{\rm ads}(\vec{r}\,') \ , \tag{3.13}$$

we get for the linear friction force (by the argument $\{\vec{r}_d\}$ we want to stress that the friction force is in principle a functional of the whole adsorbate trajectory)

$$\begin{aligned}
\vec{F}_{\rm friction}(\{\vec{r}_d\};t) &= \int_{-\infty}^{t} d\tau\, \overleftrightarrow{\mathcal{G}}(\vec{r}_d(t);t-\tau) \cdot \left(\vec{r}_d(t) - \vec{r}_d(\tau)\right) \\
&= \int_{-\infty}^{t} d\tau\, \overleftrightarrow{\mathcal{G}}(\vec{r}_d(t);t-\tau) \cdot \int_{\tau}^{t} d\xi \vec{v}_d(\xi) \\
&= \int_{-\infty}^{t} d\tau\, \overleftrightarrow{\Gamma}(\vec{r}_d(t);t-\tau) \cdot \vec{v}_d(\tau) + \overleftrightarrow{\Gamma}(\vec{r}_d(t);t-\tau) \cdot \int_{\tau}^{t} d\xi \vec{v}_d(\xi) \Big|_{\tau=-\infty}^{t} \\
&= \int_{-\infty}^{t} d\tau\, \overleftrightarrow{\Gamma}(\vec{r}_d(t);t-\tau) \cdot \vec{v}_d(\tau)
\end{aligned} \tag{3.14a}$$

with

$$\overleftrightarrow{\Gamma}(\vec{r}_d(t);t-\tau) = \int_{t-\tau}^{\infty} d\xi\, \overleftrightarrow{\mathcal{G}}(\vec{r}_d(t);\xi) \tag{3.14b}$$

being the retarded linear friction coefficient kernel which is explicitly dependent on the actual adsorbate particle position and which has in general non-zero memory. It is explicitly given by

$$\overleftrightarrow{\Gamma}(\vec{r};t) = \int_{t}^{\infty} d\tau \int d^3\vec{r}_1 \int d^3\vec{r}_2\, \rho_{\rm ads}(\vec{r}_1) \left(\nabla_{\vec{r}_1}\, \nabla_{\vec{r}_2}\, G_C^R(\vec{r}_1+\vec{r},\vec{r}_2+\vec{r};\tau)\right) \rho_{\rm ads}(\vec{r}_2) \ . \tag{3.15}$$

Thus, the friction force exerted by the substrate on the adsorbate at the position $\vec{r}_d(t)$ with the velocity $\vec{v}_d(t)$ is given by the convolution equation

$$\vec{F}_{\rm friction}(\{\vec{r}_d\};t) = \int_{0}^{\infty} d\tau\, \overleftrightarrow{\Gamma}(\vec{r}_d(t);\tau) \cdot \vec{v}_d(t-\tau) \ , \tag{3.16}$$

which may be further simplified in some special cases. First, let us consider the situation when the velocity of the adsorbate movement is changing slowly compared

with the characteristic time scale of the friction kernel, the extreme example of which is the constant velocity motion. Then we may use the *Markovian approximation* and expand $\vec{v}_d(t-\tau)$ around $\tau = 0$. This yields already in the zeroth order

$$\vec{F}_{\rm friction}(\{\vec{r}_d\};t) \approx \int_0^\infty d\tau \overleftrightarrow{\Gamma}(\vec{r}_d(t);\tau)\cdot\vec{v}_d(t) = -\overleftrightarrow{\gamma}(\vec{r}_d(t))\cdot\vec{v}_d(t)\ , \tag{3.17}$$

with the linear friction coefficient being given by

$$\begin{aligned}\overleftrightarrow{\gamma}(\vec{r}) &= -\int_0^\infty d\tau\,\overleftrightarrow{\Gamma}(\vec{r};\tau) = -\int_0^\infty d\tau\int_\tau^\infty d\xi\,\overleftrightarrow{\mathcal{G}}(\vec{r};\xi)\\ &= -\int_0^\infty d\tau\,\tau\,\overleftrightarrow{\mathcal{G}}(\vec{r};\tau) = -\lim_{\omega\to 0}\frac{d}{id\omega}\overleftrightarrow{\mathcal{G}}(\vec{r};\omega) = -\lim_{\omega\to 0}\frac{d}{d\omega}\Im\overleftrightarrow{\mathcal{G}}(\vec{r};\omega)\\ &= \int d^3\vec{r}_1\int d^3\vec{r}_2\,\rho_{\rm ads}(\vec{r}_1)\left(-\lim_{\omega\to 0}\frac{d}{d\omega}\nabla_{\vec{r}_1}\nabla_{\vec{r}_2}\Im G_C^R(\vec{r}_1+\vec{r},\vec{r}_2+\vec{r};\omega)\right)\rho_{\rm ads}(\vec{r}_2)\ .\end{aligned} \tag{3.18}$$

Second, it is possible to exactly evaluate the friction force for the harmonic motion of the adsorbate. Suppose that $\vec{v}_d(t) = \vec{v}_0\cos\omega_d t$ and $\vec{r}_d(t) = \vec{r}_0\sin\omega_d t = \frac{\vec{v}_0}{\omega_d}\sin\omega_d t$. Then the expression for the friction force may be reformulated as

$$\vec{F}_{\rm friction}(\{\vec{r}_d\};t) = \left(\overleftrightarrow{\mathcal{G}}(\vec{r}_d(t);\omega\to 0) - \Re\overleftrightarrow{\mathcal{G}}(\vec{r}_d(t);\omega_d)\right)\cdot\vec{r}_d(t) + \frac{1}{\omega_d}\Im\overleftrightarrow{\mathcal{G}}(\vec{r}_d(t);\omega_d)\cdot\vec{v}_d(t)\ . \tag{3.19}$$

The second term yields the memory-less friction force linear in velocity, while the first one (not present in the Markovian approximation) represents a reactive force which accounts for the fact that the interaction of the adsorbate with the substrate creates an effective potential for the adsorbate movement. In fact, in this case we got that adsorbate motion induces a harmonic potential, i. e. we obtained the renormalization of the lateral motion eigenfrequency from zero to a non-zero value. The steady motion case is obtained from this harmonic one by taking the limit $\omega_d \to 0$, and we see that we fully recover the Markovian results — the effective potential vanishes and the friction coefficient is again given by (3.18).

### 3.2.2 Adsorbates with quantum-fluctuating charge distributions

Now, we return to the case when both the charge distributions involved have their own quantum-mechanical dynamics (physisorption cases). In this case, we have to go back to Eq. (3.4). The mean value of the force may be expressed as

$$\begin{aligned}\vec{F}(t) = -\int_{-\infty}^t d\tau\int d^3\vec{r}\,d^3\vec{r}\,'\\ \frac{1}{i\hbar}\left\langle\left[\tilde{\rho}_{\rm ads}(\vec{r},t;\vec{r}_d(t))\,\nabla_{\vec{r}}\tilde{\phi}_{\rm sub}(\vec{r},t),\tilde{\rho}_{\rm ads}(\vec{r}\,',\tau;\vec{r}_d(\tau))\tilde{\phi}_{\rm sub}(\vec{r}\,',\tau)\right]\right\rangle\ .\end{aligned} \tag{3.20}$$

We explicitly indicated the dependence of $\tilde{\rho}_{\rm ads}(\vec{r},t;\vec{r}_d(t))$ on $\vec{r}_d(t)$ (cf. (3.1c)). The "other part" of its time dependence stems from the free quantum dynamics of the adsorbate charge governed by $\hat{H}_{\rm ads}$ in the Dirac picture. By employing (3.1c) and shifting the integration variables $\vec{r}$, $\vec{r}\,'$, we come to the formula

$$\begin{aligned}\vec{F}(t) = &-\int_{-\infty}^{t} d\tau \int d^3\vec{r}\, d^3\vec{r}\,' \\ &\frac{1}{i\hbar}\big\langle \big[\tilde{\rho}_{\rm ads}(\vec{r},t)\,\nabla_{\vec{r}}\tilde{\phi}_{\rm sub}(\vec{r}+\vec{r}_d(t),t), \tilde{\rho}_{\rm ads}(\vec{r}\,',\tau)\tilde{\phi}_{\rm sub}(\vec{r}\,'+\vec{r}_d(\tau),\tau)\big]\big\rangle\end{aligned} \tag{3.21}$$

in which the time dependence of $\tilde{\rho}_{\rm ads}(\vec{r},t)$ is exclusively due to the free quantum evolution according to $\hat{H}_{\rm ads}$ and $\langle\bullet\rangle$ means the averaging over the canonical state of free adsorbate and substrate. Now, we can repeat the expansion of the second Coulomb field around $\vec{r}_d(t)$ and, following the analogous derivation as in the previous case, we get for the friction kernel (in analogy with Eq. (3.15))

$$\begin{aligned}\overleftrightarrow{\Gamma}_{\rm fluct}(\vec{r};t) = &\int_{t}^{\infty} d\tau \int d^3\vec{r}_1\, d^3\vec{r}_2 \\ &\frac{1}{i\hbar}\big\langle \big[\tilde{\rho}_{\rm ads}(\vec{r}_1,\tau)\,\nabla_{\vec{r}_1}\tilde{\phi}_{\rm sub}(\vec{r}_1+\vec{r},\tau), \tilde{\rho}_{\rm ads}(\vec{r}_2,0)\nabla_{\vec{r}_2}\tilde{\phi}_{\rm sub}(\vec{r}_2+\vec{r},0)\big]\big\rangle\ ,\end{aligned} \tag{3.22}$$

which yields in the Markovian approximation the linear friction coefficient

$$\begin{aligned}\overleftrightarrow{\gamma}_{\rm fluct}(\vec{r}) = &-\int d^3\vec{r}_1\, d^3\vec{r}_2 \lim_{\omega\to 0}\frac{d}{d\omega}\Im\int_0^{\infty} dt e^{i\omega t}\cdot \\ &\frac{1}{i\hbar}\big\langle \big[\tilde{\rho}_{\rm ads}(\vec{r}_1,t)\,\nabla_{\vec{r}_1}\tilde{\phi}_{\rm sub}(\vec{r}_1+\vec{r},t), \tilde{\rho}_{\rm ads}(\vec{r}_2,0)\nabla_{\vec{r}_2}\tilde{\phi}_{\rm sub}(\vec{r}_2+\vec{r},0)\big]\big\rangle\ .\end{aligned} \tag{3.23}$$

To simplify further this formula, we use the identity

$$\begin{aligned}&\big[\tilde{\rho}_{\rm ads}(\vec{r},t)\,\tilde{\phi}_{\rm sub}(\vec{r}_1,t), \tilde{\rho}_{\rm ads}(\vec{r}\,',0)\tilde{\phi}_{\rm sub}(\vec{r}_2,0)\big] \\ &\qquad = \frac{1}{2}\big\{\tilde{\rho}_{\rm ads}(\vec{r},t), \tilde{\rho}_{\rm ads}(\vec{r}\,',0)\big\}\big[\tilde{\phi}_{\rm sub}(\vec{r}_1,t), \tilde{\phi}_{\rm sub}(\vec{r}_2,0)\big] \\ &\qquad + \frac{1}{2}\big[\tilde{\rho}_{\rm ads}(\vec{r},t), \tilde{\rho}_{\rm ads}(\vec{r}\,',0)\big]\big\{\tilde{\phi}_{\rm sub}(\vec{r}_1,t), \tilde{\phi}_{\rm sub}(\vec{r}_2,0)\big\}\ ,\end{aligned} \tag{3.24}$$

where $\{\bullet,\bullet\}$ denotes the anticommutator and where the commutativity of $\tilde{\rho}_{\rm ads}(\vec{r},t)$ and $\tilde{\rho}_{\rm sub}(\vec{r}\,',t')$ and thus also of $\tilde{\phi}_{\rm sub}(\vec{r}_1,t')$ has been used. Next, we perform the Fourier transform of the above equation with respect to $t$, use the convolution in

the Fourier picture, and utilize the *fluctuation-dissipation theorem*

$$\int_{-\infty}^{\infty} dt e^{i\omega t} \big\langle \big\{ \tilde{\rho}_{\rm ads}(\vec{r},t), \tilde{\rho}_{\rm ads}(\vec{r}\,',0) \big\} \big\rangle = -\frac{\hbar}{2\pi} \coth \frac{\hbar\omega}{2k_BT} \Im \chi^R_{\rho\rho}(\vec{r},\vec{r}\,';\omega)$$
$$= -\frac{\hbar}{2\pi} \coth \frac{\hbar\omega}{2k_BT} \Im \int_0^{\infty} dt e^{i\omega t} \frac{1}{i\hbar} \big\langle \big[ \tilde{\rho}_{\rm ads}(\vec{r},t), \tilde{\rho}_{\rm ads}(\vec{r}\,',0) \big] \big\rangle \tag{3.25a}$$
$$\int_{-\infty}^{\infty} dt e^{i\omega t} \big\langle \big\{ \tilde{\phi}_{\rm sub}(\vec{r}_1,t), \tilde{\phi}_{\rm sub}(\vec{r}_2,0) \big\} \big\rangle = -\frac{\hbar}{2\pi} \coth \frac{\hbar\omega}{2k_BT} \Im G^R_C(\vec{r}_1,\vec{r}_2;\omega)$$
$$= -\frac{\hbar}{2\pi} \coth \frac{\hbar\omega}{2k_BT} \Im \int_0^{\infty} dt e^{i\omega t} \frac{1}{i\hbar} \big\langle \big[ \tilde{\phi}_{\rm sub}(\vec{r}_1,t), \tilde{\phi}_{\rm sub}(\vec{r}_2,0) \big] \big\rangle \tag{3.25b}$$

which connects the anticommutator response (fluctuations) with the imaginary part of the commutator response (dissipation). Thus, we obtain

$$\overleftrightarrow{\gamma}_{\rm fluct}(\vec{r}) = \frac{\hbar}{4\pi} \int d^3\vec{r}_1\, d^3\vec{r}_2 \lim_{\omega\to 0} \frac{d}{d\omega} \Im \int_{-\infty}^{\infty} \frac{d\Omega}{2\pi}$$
$$\Big( \coth \frac{\hbar\Omega}{2k_BT} \Im \chi^R_{\rho\rho}(\vec{r}_1,\vec{r}_2;\Omega) \nabla_{\vec{r}_1} \nabla_{\vec{r}_2} G^R_C(\vec{r}_1+\vec{r},\vec{r}_2+\vec{r};\omega-\Omega) \tag{3.26}$$
$$+ \coth \frac{\hbar(\omega-\Omega)}{2k_BT} \chi^R_{\rho\rho}(\vec{r}_1,\vec{r}_2;\Omega) \nabla_{\vec{r}_1} \nabla_{\vec{r}_2} \Im G^R_C(\vec{r}_1+\vec{r},\vec{r}_2+\vec{r};\omega-\Omega) \Big) \ .$$

The integral over auxiliary frequencies may be changed into the integral over positive (physical) frequencies only, yielding

$$\lim_{\omega\to 0} \frac{d}{d\omega} \Im \int_{-\infty}^{\infty} \frac{d\Omega}{2\pi} \Big( \coth \frac{\hbar\Omega}{2k_BT} \Im \chi^R_{\rho\rho}(\vec{r}_1,\vec{r}_2;\Omega) \nabla_{\vec{r}_1} \nabla_{\vec{r}_2} G^R_C(\vec{r}_1+\vec{r},\vec{r}_2+\vec{r};\omega-\Omega)$$
$$+ \coth \frac{\hbar(\omega-\Omega)}{2k_BT} \chi^R_{\rho\rho}(\vec{r}_1,\vec{r}_2;\Omega) \nabla_{\vec{r}_1} \nabla_{\vec{r}_2} \Im G^R_C(\vec{r}_1+\vec{r},\vec{r}_2+\vec{r};\omega-\Omega) \Big)$$
$$= \lim_{\omega\to 0} \frac{d}{d\omega} \int_0^{\infty} \frac{d\Omega}{2\pi} \Big( \coth \frac{\hbar\Omega}{2k_BT} \Im \chi^R_{\rho\rho}(\vec{r}_1,\vec{r}_2;\Omega) \big[ \nabla_{\vec{r}_1} \nabla_{\vec{r}_2} \Im G^R_C(\vec{r}_1+\vec{r},\vec{r}_2+\vec{r};\omega-\Omega)$$
$$+ \nabla_{\vec{r}_1} \nabla_{\vec{r}_2} \Im G^R_C(\vec{r}_1+\vec{r},\vec{r}_2+\vec{r};\omega+\Omega) \big] + \Im \chi^R_{\rho\rho}(\vec{r}_1,\vec{r}_2;\Omega) \cdot$$
$$\big[ \coth \frac{\hbar(\omega-\Omega)}{2k_BT} \nabla_{\vec{r}_1} \nabla_{\vec{r}_2} \Im G^R_C(\vec{r}_1+\vec{r},\vec{r}_2+\vec{r};\omega-\Omega)$$
$$- \coth \frac{\hbar(\omega+\Omega)}{2k_BT} \nabla_{\vec{r}_1} \nabla_{\vec{r}_2} \Im G^R_C(\vec{r}_1+\vec{r},\vec{r}_2+\vec{r};\omega+\Omega) \big] \Big)$$
$$= 2 \int_0^{\infty} \frac{d\Omega}{2\pi} \Big( -\frac{d}{d\Omega} \coth \frac{\hbar\Omega}{2k_BT} \Big) \Im \chi^R_{\rho\rho}(\vec{r}_1,\vec{r}_2;\Omega) \nabla_{\vec{r}_1} \nabla_{\vec{r}_2} \Im G^R_C(\vec{r}_1+\vec{r},\vec{r}_2+\vec{r};\Omega) \ . \tag{3.27}$$

In the derivation, we made use of the property that the imaginary parts of retarded responses are odd functions of the frequency. Finally, we may summarize our result

for the fluctuational friction coefficient

$$\overleftrightarrow{\gamma}_{\mathrm{fluct}}(\vec{r}) = \frac{\hbar}{2\pi}\int_0^\infty \frac{d\Omega}{2\pi}\Big(-\frac{d}{d\Omega}\coth\frac{\hbar\Omega}{2k_BT}\Big)\int d^3\vec{r}_1\, d^3\vec{r}_2 \\ \Im\chi^R_{\rho\rho}(\vec{r}_1,\vec{r}_2;\Omega)\nabla_{\vec{r}_1}\nabla_{\vec{r}_2}\Im G^R_C(\vec{r}_1+\vec{r},\vec{r}_2+\vec{r};\Omega)\ . \tag{3.28}$$

## 3.3 Review of results

Now, we will utilize the obtained results to illustrate their usage for various physical set-ups. Namely, we will present several different treatments found in the literature from our unifying point of view and will give the examples of results for the corresponding friction coefficients. Different approaches to the electronic friction use different choices of the charge distributions and/or approximations to evaluate the response functions. First, let us consider the case of point-like adsorbates with either classical or quantum-fluctuating charge distributions. Such situations were studied in the context of a Brownian motion model of an ion above a jellium substrate (Schaich [27] and Ferrell et al. [28]), for ions and atoms above jellium treated by the density functional (Liebsch [29]), for a normal metal substrate with impurities (Tomassone and Widom [26]), and then for a superconducting substrate (Novotný and Velický [30] and Sokoloff et al. [31]). The adsorbate charge distributions considered in the paper by Tomassone and Widom [26] were: an ion with the charge $Ze$, a point-like classical dipole with the dipole moment $\vec{p}$, and finally an atom with the fluctuating quantum mechanical dipole with the polarizability $\overleftrightarrow{\alpha}(\omega)$. The respective friction coefficients are then given simply by

$$\overleftrightarrow{\gamma}^{(\mathrm{Z})}(\vec{r}) = -Z^2e^2\lim_{\omega\to0}\frac{d}{d\omega}\lim_{\vec{r}\to\vec{r}\,'}\nabla_{\vec{r}}\,\nabla_{\vec{r}\,'}\,\Im G^R_C(\vec{r},\vec{r}\,';\omega)\ , \tag{3.29a}$$

$$\overleftrightarrow{\gamma}^{(\vec{p})}(\vec{r}) = -\lim_{\omega\to0}\frac{d}{d\omega}\lim_{\vec{r}\to\vec{r}\,'}\nabla_{\vec{r}}\,\nabla_{\vec{r}\,'}\,(\vec{p}\cdot\nabla_{\vec{r}})(\vec{p}\cdot\nabla_{\vec{r}\,'})\Im G^R_C(\vec{r},\vec{r}\,';\omega)\ , \tag{3.29b}$$

$$\overleftrightarrow{\gamma}^{(QM)}(\vec{r}) = \frac{\hbar}{2\pi}\int_0^\infty\frac{d\Omega}{2\pi}\Big(-\frac{d}{d\Omega}\coth\frac{\hbar\Omega}{2k_BT}\Big) \\ \lim_{\vec{r}\to\vec{r}\,'}\nabla_{\vec{r}}\cdot\Im\overleftrightarrow{\alpha}(\Omega)\cdot\nabla_{\vec{r}\,'}\nabla_{\vec{r}}\nabla_{\vec{r}\,'}\Im G^R_C(\vec{r},\vec{r}\,';\Omega)\ . \tag{3.29c}$$

These results are essentially identical in all the papers even though the approaches, derivations, and the formalisms used are different. It remains to calculate the Coulomb Green's function which microscopically describes the surface response of the substrate to a perturbation caused by the adsorbate movement. This is the central task in the solution of the problem.

In the paper by Tomassone and Widom [26], a simple phenomenological form of the surface response of a flat metal substrate was used. Namely, the substrate properties were modeled by approximating the Coulomb Green's function in the

*image-charge form*, reading

$$G_C^R(\vec{r},\vec{r}';\omega) = -\frac{\varepsilon(\omega)-1}{\varepsilon(\omega)+1}\frac{1}{R_{\text{image}}} \tag{3.30}$$

with $R_{\text{image}} = |\vec{r}-\vec{r}'_{\text{image}}|$, where $\vec{r}'_{\text{image}}$ is the mirror image of $\vec{r}'$ made by the (flat) surface plane and $\varepsilon(\omega)$ is the local permitivity of the substrate. It can be expressed in terms of the local conductivity as

$$\varepsilon(\omega) = 1 + \frac{i\sigma(\omega)}{\omega\varepsilon_0} \ . \tag{3.31}$$

In this approximation, we get in the case of the lateral motion of the adsorbate in the height $h$ above a normal metal ($\sigma(\omega) \equiv \sigma = \text{const}$) considered in [26] for the lateral friction coefficient of an ion

$$\gamma_{\parallel}^{(\text{Z})}(h) \equiv \gamma_{xx}^{(\text{Z})}(h) = \gamma_{yy}^{(\text{Z})}(h) = \frac{Z^2e^2\varepsilon_0}{4\sigma h^3} \ . \tag{3.32}$$

The permanent and quantum-fluctuating dipole cases are evaluated in a similar manner yielding more complicated formulas found in [26].

The image-charge form of the Coulomb Green's function was also used in the treatment of the van der Waals friction above superconducting substrate motivated by the measurements by Krim et al. In this case, the simple two-fluid model of the superconductor response was employed, yielding the sudden drop of friction coefficient at the critical temperature. We will present a more detailed discussion on this topic in the next section of this chapter.

In other papers, a more fundamental approaches to the evaluation of the surface response were chosen. Schaich [27] and Liebsch [29] used the jellium model with a surface and calculated the surface response, using the RPA and time-dependent density functional theory, respectively. Yet another method was employed by Ferrell et al. [28]. They evaluated the surface response of the substrate from a non-local bulk dielectric function, using the specular reflection model.

In any case, for a flat surface, i. e. laterally translationally invariant, of the substrate occupying the halfspace $z \leq 0$, we can write with the help of $V_C(q,z,z') = \frac{2\pi}{q}e^{-q|z-z'|}$ for the lateral Fourier transform of the Coulomb Green's function (3.7a)

$$G_C^R(q,z,z';\omega) = -\frac{2\pi}{q}e^{-q(z+z')}g(q;\omega) \tag{3.33}$$

with

$$g(q;\omega) = -\frac{2\pi}{q}\int d^2\vec{r}_{\parallel}\int_{-\infty}^{0}dz\int_{-\infty}^{0}dz'e^{qz+qz'-i\vec{q}\cdot\vec{r}_{\parallel}}\chi(\vec{r}_{\parallel},z,z';\omega) \tag{3.34}$$

being the surface response function [32, 33, 29]. Then the result (3.29) for the friction coefficient of, e. g. an ion above the surface can be reformulated in the following manner

$$\gamma_{\perp}^{(\mathrm{Z})}(h) = Z^2 e^2 \lim_{\omega \to 0} \frac{1}{\omega} \int_0^{\infty} dq q^2 e^{-2qh} \Im g(q;\omega) \ , \tag{3.35}$$

$$\gamma_{\parallel}^{(\mathrm{Z})}(h) = \frac{\gamma_{\perp}^{(\mathrm{Z})}(h)}{2} \ . \tag{3.36}$$

The knowledge of the surface response function is thus sufficient for determining the microscopic friction coefficient. Its calculation is quite a difficult numerical task even in the simplest possible model consisting of a jellium surface [32, 29]. However, it is possible to make reasonable approximations for it. The simplest one consist in replacing its values by its long-wavelength limit ($q \to 0$) only. In this approximation the surface response reduces to the familiar image-charge form of Tomassone and Widom [26]

$$g_{IC}(q;\omega) \approx \lim_{q \to 0} g(q;\omega) = \frac{\varepsilon(\omega) - 1}{\varepsilon(\omega) + 1} \ . \tag{3.37}$$

This approximation is precise for the substrate with a local dielectric function $\varepsilon(\omega)$. Another approximation used for the surface response function is that of *specular reflection model* [28, 34, 33]

$$g_{SR}(q;\omega) = \frac{1 - \varepsilon_s(q;\omega)}{1 + \varepsilon_s(q;\omega)} \tag{3.38}$$

with

$$\varepsilon_s(q;\omega) = \frac{q}{\pi} \int_{-\infty}^{\infty} dk_z \frac{1}{(k_z^2 + q^2)\varepsilon(\vec{k};\omega)} \ , \tag{3.39}$$

where $\varepsilon(\vec{k};\omega)$ is the bulk dielectric response of the substrate (generally non-local, i. e. $\vec{k}$-dependent). Again, for the local bulk permitivity we recover the image-charge limit.

A second kind of charge distributions considered is that of charge fluctuations in a bulk slab above the substrate [35, 36, 37, 38]. Such models of van der Waals friction between two closely spaced solids are often used to model macroscopic friction between macroscopic objects. However, the relevance of these models for the macroscopic friction is indeed little as discussed by Persson and Zhang [37], and they rather serve as a playground for theorists of friction to develop and check the suitable techniques. As pointed out by Persson and Zhang in [37], there are physically relevant contexts in which these models play a role, namely, the cases of the *Coulomb drag* between two parallel electron systems in semiconducting nanostructures and

the QCM experiments. In the latter case, the physisorbed thin film experiences a non-zero friction force stemming from the dissipative part of the fluctuational interaction between the film and substrate charge densities (cf. (3.28)). Contrary to the macroscopic case, this source of friction force is relevant and usually comparable with the other sources of the microscopic friction, e. g. interaction with substrate phonons and dissipation into the film degrees of freedom. It should be noted that the linear response theory developed in the previous text is not sufficient to describe the friction force between two macroscopic bodies. At least the mutual screening of the charge fluctuations in the respective bodies must be included by going to higher orders in the perturbation theory. Since an infinite number of contributions must be summed, non-perturbative approaches are usually used [35, 36, 38]. Also not only the linear friction coefficient is considered but the whole velocity dependence of the friction force is explored. In spite of all these differences, the presented approach has many analogies with the non-perturbative methods.

There are other cases when the linear response regime is not sufficient for the description of the microscopic friction. These cover the physically relevant cases of the friction of the physisorbed layers. From (3.28) we see that the friction coefficient on an adsorbed film is proportional to $\Im\chi^R_{\rho\rho}(\vec{r}_1, \vec{r}_2; \Omega)$, the imaginary part of the polarizability of the film. In the case of a model study for one atom, it is the polarizability of the atom. For small enough temperatures $\frac{d}{d\Omega} \coth \frac{\hbar\Omega}{2k_BT}$ acts as an approximate delta-function with the halfwidth $\approx \frac{k_BT}{\hbar}$. Thus, if the excited states of the film have the energy high above the temperature which is typical for physisorbed atoms, the first order (linear response) contribution is exponentially small and one has to consider the second-order term. It would be possible to continue in the perturbation expansion of (3.3) and to evaluate the linear friction coefficient in analogy with the first-order term. This is, however, too involved to be presented here. Instead, we only refer to two papers where the problem of a physisorbed atom was questioned. Sokoloff [13] and Persson and Volokitin [39] found that the second-order term yields a finite contribution to the friction coefficient proportional to the square of the static atomic polarizability. Moreover, Persson and Volokitin [39] showed that the response of the surface to the quantum fluctuations of the atomic dipole can be approximated by the surface response function introduced above. Thus, our previous discussion of the surface response and its approximations can be equally used in this more complicated case of physisorbed atoms.

## 3.4 Friction above superconducting substrate

Now, let us turn our attention to a special case of the electronic friction problem, namely, to the electronic friction above the superconducting surface. As was already mentioned, this model is inspired by the recent findings by Krim and collaborators

[14] who found that the friction coefficient experiences a sudden drop at the transition point. Their naive interpretation, assuming that the electronic degrees of freedom simply decouple due to the SC transition, was contested by Persson and Tosatti [15]. Persson and Tosatti claimed that the friction is caused by the dissipation into the normal fluid in the superconductor and, thus, should decrease continuously in accord with the continuous decrease of the normal fluid density with temperature. No sharp drop observed should be present according to Persson and Tosatti. The tentative explanations of the puzzle raised by them were given by Popov [40], Novotný and Velický [30] and Sokoloff et al. [31]. All of them use some phenomenological arguments so that neither of them gives the final answer to the problem, but, on the other hand, all of them proved that the argumentation of Persson and Tosatti is highly questionable. In all these contributions, the peculiar features of the superfluid component of the electron density in the superconductor turned out to play the dominant role. We will present here the reasoning by Novotný and Velický and then will briefly comment on the other two works.

Let us consider an ion oscillating with the external driving frequency $\omega_d$ above a substrate which may be made superconducting. The friction force on the ion is then given by an analogy of equation (3.29a) stemming from (3.19)

$$\overset{\leftrightarrow}{\gamma}^{(\mathrm{Z})}(\vec{r},\omega_d) = -Z^2e^2\frac{1}{\omega_d}\lim_{\vec{r}\to\vec{r}'}\nabla_{\vec{r}}\nabla_{\vec{r}'}\,\Im G_C^R(\vec{r},\vec{r}';\omega_d)\ . \tag{3.40}$$

We use the image-charge approximation (3.30) for the Coulomb Green's function, which is the point where the phenomenology enters the reasoning. The equation (3.31) is again used to express the permitivity via the conductivity of the substrate. We omit all the spatial dependence of the Green's function as we are only interested in the temperature dependence of the friction coefficient which depends exclusively on the factor

$$\gamma^{\mathrm{Z}}(\omega_d) \propto \frac{1}{\omega_d}\Im\frac{\varepsilon(\omega_d)-1}{\varepsilon(\omega_d)+1}\ . \tag{3.41}$$

Now, we proceed to analyze the effect of the superconducting transition on this factor, and, thus, on the friction force. First, we evaluate the conductivity of the substrate in the simple two-fluid model of the superconductor. In this model, the conductivity consists of two additive terms, the first one due to the superfluid component and the other one due to the normal fluid component

$$\sigma(\omega) = \sigma_S(\omega) + \sigma_N(\omega)\ . \tag{3.42}$$

Denoting by $x$ the ratio of the density of normal electrons to the total electron density, $x = \frac{n_N}{n}$, we may use (3.42) both above ($x = 1$) and below ($x < 1$) the phase transition. We also use notations $m^*$ for the effective mass of the electrons and $\omega_{pl}$ for the electron plasma frequency in the substrate, $\omega_{pl}^2 = \frac{ne^2}{\varepsilon_0 m^*}$. The superfluid

component experiences no friction force due to disorder and its long-wave limit behaves like

$$\sigma_S(\omega) = \frac{i n_S e^2}{m^* \omega} = i(1-x)\varepsilon_0 \frac{\omega_{pl}^2}{\omega} \ . \tag{3.43}$$

The normal fluid is assumed to satisfy the Drude formula for the AC conductivity, with the proper electron density $x\,n$, both below and above $T_c$:

$$\sigma_N(\omega) = \frac{n_N e^2 \tau}{m^*} \frac{1}{1 - i\,\omega\tau} \doteq \frac{n_N e^2 \tau}{m^*} = x\varepsilon_0 \omega_{pl}^2 \tau \ . \tag{3.44}$$

The relaxation time in the Drude formula is limited by phonon and disorder related scattering and may then be bracketed between $10^{-14}s$ and $10^{-11}s$ (corresponding to pure lead at 300 K and 7 K). Since the experimental setup is a quartz crystal microbalance arrangement with the driving frequency being roughly $\omega_d \approx 10^7 s^{-1}$, we use the DC limit of the normal conductivity, $\omega = 0$, neglecting thus its frequency dependence.

Introducing the conductivity (3.42) into (3.41), with the help of (3.31) we obtain an explicit result for the linear friction coefficient

$$\Gamma(x, \omega_d) \propto \frac{2}{\omega_{pl}^2 \tau} \frac{x}{x^2 + \left(\frac{1-x-2(\omega_d/\omega_{pl})^2}{\omega_d \tau}\right)^2} \doteq \frac{2}{\omega_{pl}^2 \tau} \frac{x}{x^2 + \left(\frac{1-x}{\omega_d \tau}\right)^2} \ . \tag{3.45}$$

The small term $\omega_d^2/\omega_{pl}^2 \approx (10^7 s^{-1}/10^{15} s^{-1})^2$ has been neglected as it does not change the results. Temperature enters this expression in two different ways. Firstly, the relaxation time $\tau$ and the plasma frequency $\omega_{pl}$ are slightly temperature dependent, yielding a moderate temperature dependence of the friction coefficient in the normal state. Around the transition point, these parameters have a smooth temperature dependence and in the close vicinity of $T_c$ they are approximately constant. Secondly, and more importantly, temperature enters the above result (3.45) through the variation of $x$, the fractional normal fluid density, with temperature. To obtain this temperature dependence around the transition point, we may employ the Ginsburg-Landau description. The lead film in the actual experiment [14] was about 1500 Å thick. Thus, it is bracketed by the Pippard and the GL coherence lengths:

$$\xi_0 \approx 830 \mathring{A} \ < \text{ film thickness } \ll \xi(T) \sim \xi_0 \Big(\frac{T_c}{T_c - T}\Big) \tag{3.46}$$

for $0 < T_c - T \ll T_c$. Under these conditions, the GL theory leads to a simple result [41], namely, that the superfluid density is constant across the width of the film and has the same temperature dependence as in the bulk. For definiteness, we assume this temperature dependence to be of the simple, yet qualitatively correct Gorter-Casimir form [42] $n_S(T)/n = 1 - x(T) = 1 - (T/T_c)^4$. We introduce this relation

into (3.45) and obtain the final dimension-less relation for the friction coefficient at $T$ close below the transition point

$$\frac{\Gamma(T,\omega_d)}{\Gamma_0} \doteq \frac{1}{1+\left(\frac{4(1-T/T_c)}{\omega_d\tau}\right)^2} = \frac{1}{1+\left(\frac{t}{\Delta t}\right)^2} \tag{3.47}$$

with $t = (T_c - T)/T_c$ and the halfwidth of the jump $\Delta t = \frac{\omega_d\tau}{4}$. By $\Gamma_0$ we have denoted the approximately constant value of the friction in the normal state just above the critical temperature. The halfwidth of the jump depends on the value of $\tau$. For a "typical" $\tau \approx 10^{-12}s$, it is of the order $10^{-5}$. This represents a smooth, but a very steep step. This is fully consistent with the experimental results of Krim and collaborators [14].

Sokoloff et al. [31] used the same approximation of the superconducting surface response in the form of the image-charge. However, they used a different method to evaluate the friction force. In fact, they did not calculate the linear friction coefficient, but a non-linear (in constant velocity) friction force. The first non-zero contribution in the superconducting state is the cubic one. Its value is considerably smaller than that in the normal state when $\frac{n_S}{n_N} \gg 10^{-6}$. This roughly corresponds to our results, proving thus that the phenomenon found by us is not an artifact of the linear response regime. The physical key point of both the methods lies in the usage of the image-charge form of the surface response. From this form, we can easily see where the reasoning of Persson and Tosatti is invalid. They simply neglected the screening of the Coulomb interaction between the adsorbate and substrate which is highly enhanced in the superconducting state by the appearance of the superfluid. The superfluid screening capabilities are so high that even in the tiny concentration, i. e. just slightly below $T_C$, the interaction of the adsorbate with the substrate is almost completely screened out and, thus, the friction force drops out. The rest of the measured friction coefficient is then attributed to the phononic contribution to friction.

Another approach was taken by Popov [40]. He used a phenomenological hydrodynamic description of the electronic fluid. The electronic fluid was considered as a viscous fluid and the interaction with the adsorbate was modeled by the boundary condition, imposing the surface drag velocity being equal to the velocity of the adsorbate movement. Both these assumptions are rather questionable, however, this model reproduces the drop in the friction coefficient correctly. The surface drag of the electron fluid together with the overall charge neutrality of the substrate imply the existence of the bulk electric current backflow. The dissipative properties of the backflow changes suddenly with the phase transition. Namely, in the superconducting state the backflow is exclusively of the supercurrent origin and, thus, does not contribute to the dissipation of the energy in the substrate and reduces the friction force.

In a recent preprint, Persson [43] argues against the proposed explanations of the drop in superconducting friction. He refuses the Popov's model as inadequate and also argues against the image-charge ansatz. He does not claim that the image-charge approximation would be in principle wrong, but he questions its relevance for the experimental findings. This is a legitimate question as the applicability of the image-charge to the superconducting surface is indeed an unresolved problem. Persson contrasts the so called *bulk contribution* (image-charge) with the so called *surface contribution* ($q$-dependent part of the surface response) and claims that the surface one is dominant by a factor of about 100–1000 for the Krim's experiment setup. The surface contribution does not undergo the sharp drop with temperature at the transition point. Thus, the findings by Krim are, according to Persson, still an open puzzle. However, his reasoning is not totally convincing as he uses expressions for the surface contribution calculated for the jellium model [32] and assumes the additivity of the bulk and surface contributions. Neither of these two assumptions is indeed justified for the superconducting substrate.

## 3.5 Concluding remarks

In this chapter, we presented the linear response theory of the electronic friction force due to the Coulomb interaction of the adsorbate and substrate charge densities. This friction force is associated with the attractive part of the adsorption bond in the physisorption and ionic cases. We considered separately both these cases which differ in the dynamics of the adsorbate charge density. Namely, in the ionic case the charge density of the adsorbate is considered to be a fixed classical one, while in the physisorption case it has its own quantum dynamics. Both these cases were treated in an unified framework of the linear response theory and a partial survey of the published results on this topic was given from the point of view of this unifying method.

In analogy with the phononic case studied in the previous chapter, the most relevant quantity for the evaluation of the microscopic friction coefficient turns out to be the retarded Green's function of the charge density fluctuations of the substrate. Contrary to the phononic case, this Green's function cannot be calculated exactly as it is a 2-particle Green's function and, thus, its evaluation for the interacting electrons in the substrate is a non-trivial task. Several expressions for this Green's function of the normal metal described by various approximations were briefly reviewed. The realistic numerical calculations of this quantity are surely at the front-end of the present methods since it is a *dynamical response* of the surface. The importance of the surface properties is exemplified by the study of the friction force above a superconducting surface presented in the previous section.

The explanation of the striking phenomenon of the sudden drop of the friction

coefficient under the superconducting critical temperature is still an open problem. We presented several phenomenological explanations of these experimental results together with the objections against them. This recent controversy about the superconducting friction problem shows a clear lack of a truly microscopic theory of this phenomenon that would be without phenomenological entries. Persson's preprint goes in this direction, but the method used is still rather phenomenological since no true microscopic calculations for an model adequate to the experiment were done. This is definitely the task for the future. However, the truly microscopic theory of the Coulomb friction above a superconducting surface which consists in at least model evaluation of the surface response function (3.34) for the superconducting surface is enormously difficult to develop. No real progress in this has been done yet.

Some simplified models for which the calculation of the surface response function could be viable are being considered. These are mainly related to the Hubbard model, describing the strongly correlated systems in which the superconducting phase as well as various magnetic phases can be achieved by a suitable choice of the local spin coupling. Within these models, it could be possible to evaluate the surface response function, using some approximations which are under control or even achieve the direct numerical solution with the present computational techniques. The Hubbard model is of interest also for its magnetic phases. The behaviour of the friction coefficient above such a magnetic substrate with respect to the phase transition in the substrate is an interesting counterpart of the superconducting friction studied and discussed above. It would be important if experiments with friction above other kinds of strongly correlated systems like, e. g. magnetic materials, were performed.

In any case, the superconducting friction problem, in spite of its complexity, opened an interesting new area of possible experimental and theoretical progress of understanding the microscopic electronic friction mechanisms. The field is open and promises many new relevant and interesting results.

# Chapter 4

# Direct methods in non-stationary stochastic problems in surface physics

## 4.1 Formulation of the problem

The model presented in this chapter was developed by the author and Doc. Petr Chvosta to extend the paradigmatic model in the realm of resonant activation by Doering and Gadoua to non-Markovian types of additional noise.

This work was motivated by the effort to analytically solve the Langevin-like stochastic equations of motion of the kind of (1.3) which are used to describe the QCM experiment. A single adatom physisorbed above the vibrating jellium surface experiences the stochastic Langevin force (1.4) from the substrate degrees of freedom and the deterministic harmonic inertial force due to the vibrations of the substrate. In a typical QCM, setup the acceleration term in the equation of motion is negligible compared to the friction term and, thus, the customary overdamped regime approximation can be used. The evaluation of the transport properties of such a system is then the aim of the calculations. For a flat surface the problem is easily solved. However, when either the corrugation of the potential or boundary conditions are taken into account, the systems exhibits highly non-trivial behaviour. The potential corrugation leads to the phenomenon called the *stochastic resonance* while incorporating of various boundary conditions (corresponding, for example, to the presence of terrace steps on the surface) generates related phenomena as the *coherent stochastic resonance* (a table-like terrace) or the *resonant activation* (two terrace steps). In all these phenomena, the transport properties (the signal-to-noise ratio for the stochastic resonance or the mean exit time for the other two) exhibit non-monotonic dependence on the frequency of the driving force. This proves the correlation of the transport properties with the driving force.

The choice of the potential corrugation or the boundary conditions picks up the particular problem. We decided to use the boundary conditions considered by Doering and Gadoua [44] which lead to the resonant activation phenomenon. The model of Doering and Gadoua consists of the diffusion on 1-dimensional segment in the linear potential fluctuating between two opposite slopes with the reflexing boundary condition at one end and the absorbing boundary condition at the other. The fluctuations of the potential are determined by the Markovian dichotomous noise. The *mean first passage time* (sometimes also called the *mean exit time*) of the absorption process was studied with a non-trivial result for the its dependence on the mean switching rate of the potential fluctuations. The mean first passage time versus mean switching rate curve exhibits a minimum which is a signature of the *noise-induced enhancement of the absorption process*. This phenomenon was first reported in the paper by Doering and Gadoua in 1992 [44] and was named by them the *resonant activation*. Since then the phenomenon was studied intensively [45]. However, the models used to study the escape over fluctuating barriers in the context of the resonant activation employ almost exclusively simple Markovian noises simulating the barrier fluctuations [44, 46, 47, 48]. On the other hand, in the coherent stochastic resonance problems the additional "noise" is actually the deterministic harmonic signal, which is for the technical reasons approximated by the multistep process [49, 50, 51]. Thus, the harmonic driving may be regarded as a special case of the non-Markovian process.

Being aware of these facts, we wanted to extend the resonant activation paradigm to the non-Markovian potential-fluctuation cases presumably of the harmonic driving origin like in the coherent stochastic resonance context. To this end, we employed the method of the *construction of trajectories* developed by Chvosta and Reineker [52] for all non-Markovian process generated by arbitrary renewal processes. This method enables to study not only the harmonic noises, but also any other ones generated by renewal processes. The original case by Doering and Gadoua [44] is recovered for the Markovian dichotomous noise. The generalization of the paper by Chvosta and Reineker [52] in this work consists in the extension of the formalism to the spatially-resolved diffusion, which is a non-trivial task.

In our study, we developed the general formalism for the description of the resonant activation in the potentials whose fluctuations are generated by general renewal process and, thus, are in general non-Markovian. The distinctive features of the approach contrasted to the customary methods usually employed in the resonant activation context are summarized in the next section. The results of our work are reprinted in Appendix C in the form of a preprint submitted to the Physical Review E.

## 4.2 Comments to Appendix C

In this section, we just want to make several comments on the method used in the paper and the results obtained there with respect to the so far known facts. Since the paper is somewhat technical, we would like to stress the new relevant contributions made by us and compare them with the present state of the art of the branch.

- In order to generalize the original model by Doering and Gadoua [44] for a non-Markovian switching, it was necessary to use a completely different method so far not used in the context of the resonant activation. This method is the extension of the construction of trajectories method developed by Chvosta and Reineker [52] to the spatially resolved diffusion problems. An adequate presentation and analysis of the method and its exemplification in the given physically relevant context is an integral part of the work. Our technique opens up for the first time a path to answering: " ... the question of both quantitative and qualitative effects of other potential shapes and/or fluctuation statistics" of Doering and Gadoua.

- This newly developed method gives new non-trivial results even in the Markovian case studied already by Doering and Gadoua. Only the mean-first-passage-time was analytically evaluated in their paper, while other quantities were considered using Monte Carlo simulations. We were able to get a fully analytic result for the channel-filling process. To our knowledge, for the first time in the literature. Moreover, the same effective method permits to characterize the channel-filling process analytically or semi-analytically even for a non-Markovian switching.

- New results were obtained for the non-Markovian potential-switching cases. We found that the resonant activation phenomenon is quite stable with respect to the change of the properties of the potential-fluctuating process. Namely, in all cases of potential-switching generated by renewal processes with the waiting time distributions having the first two moments, the resonant activation phenomenon was preserved. The harmonic driving was in our study approximated by the deterministic two-state process and the resonant activation minimum was developed the best in this case compared to all other considered potential-fluctuation processes. Thus, we may conclude that the resonant activation phenomenon should be present in the QCM setup if the surface morphology could be approximated by the appropriate boundary conditions.

- For potential-fluctuating processes generated by renewal processes with the waiting time distributions without the second or even the first moment, the

resonant activation phenomenon disappears. Since the distributions without moments are quite common in nature, as exemplified by the *Lévy flights* [53], this finding could be relevant in some physical or biological contexts. An analogous result for a different kind of models was found by Barkai and Fleurov [54, 55].

- Our method is very general and permits many physically relevant extensions to related fields. As mentioned in the text, a generalization to more complicated potential profiles is straightforward. Changing the boundary conditions imposed on the diffusion in the safe domain, we may use it directly to study the current problems of coherent stochastic resonance and their generalizations. Any exotic non-Markovian switching time distributions may be used in our method, some of them even permitting a fully analytic solution.

# Chapter 5

# Conclusions

In this work, we considered three particular problems of the microscopic theory of friction motivated by the QCM experiment by J. Krim. The problems concern the evaluation of the respective contributions to the microscopic friction force and the solution of the stochastic equation of motion of the adsorbates on the vibrating surface of the microbalance.

In the first part devoted to the evaluation of the phononic contribution to the friction coefficient, we found the friction force and the effective equation of motion for an adatom harmonically pinned above an oscillating harmonic lattice. We generalize the models studied previously by Persson and Rydberg [17], and Georgievskii et al. [18] to the QCM setup involving the vibrations of the substrate. Two methods of solution were employed. The phenomenological one gave us correctly the friction coefficient, while the more sophisticated perturbative projection technique provided us with the full equation of motion of the adatom. The phenomenological results for the friction coefficient were confirmed by the projection technique. As the most important quantity was identified the retarded Green's function of the phononic field which was evaluated in Appendix A using a non-standard method motivated by the surface Green's function technique [56]. This evaluation, together with the new results for the equation of motion of the adatom above the vibrating substrate may be considered as new original contributions of this part of the work.

In the second part, we studied the electronic contribution to the microscopic friction coefficient due to the long range Coulomb interaction. A unifying approach within the framework of the linear response theory is presented, and from this general point of view, most of the results published so far on this problem are rederived and summarized. We present here a theory for both the adsorbates with classical charge distributions (corresponding to the ionic adsorption bond) and the adsorbates with quantum fluctuating charge distributions (van der Waals coupling), in the first order of perturbation theory. The relevance of higher order contributions is

also briefly discussed. Further, we discuss the results found in the literature about the electronic friction force above normal metal surfaces and, in particular, several approximations to the surface response are compared. The original results of this section consist in the evaluation of the electronic friction force for an adsorbate above a superconducting surface. This was measured by Krim et al. [14] and may be of a direct importance for the separation of the phononic and electronic contributions to the friction force. We suggest a tentative explanation of the experimental findings and contrast it with work of other authors on this topic. The published paper on this topic by the author [30] is reprinted in Appendix B.

In the third part, a stochastic model of the surface diffusion on a vibrating substrate is introduced and solved. The model exhibits the phenomenon called resonant activation first reported by Doering and Gadoua [44]. We extended their model to the non-Markovian potential-switching processes. The method used for solution as well as the results achieved form an original contribution by the author. The preprint submitted to Phys. Rev. E is reprinted in Appendix C.

All the models considered can be further developed to better describe the physically relevant situations. Namely, the phononic friction model introduced in the first part may be improved by taking into account a realistic washboard-like surface potential in which the adatom moves and the discrete nature of the substrate. Such a generalization would be directly related to the QCM experimental results for highly submonolayer coverages.

The problem of the superconducting friction is still open and there is an ultimate need of the microscopic theory of this phenomenon. Also other strongly correlated surfaces (e. g. magnetic) are interesting from both the experimental and theoretical point of view. Moreover, the theory which would incorporate both the lattice and electronic contributions in a unified formalism should be finally developed. All these questions promise to open wide ranges of theoretical research of the microscopic friction phenomena.

The stochastic model from the third part can be further extended in many ways as described in detail in the main text. Because of its rather abstract nature, it could be used as a basis for more specific models relevant in much broader range of situations than in the surface science only, including biophysical, chemical and biological applications.

To sum up, we believe that the problems discussed and solved in this work enrich the theory of microscopic friction and that they show the ways to further developments in this research area. The author hopes that the reader will find the topics presented here interesting and stimulating for his or her scientific work.

# Bibliography


[1] F. P. Bowden and D. Tabor. *Friction and Lubrication.* Methuen, London, 1967.

[2] B. N. J. Persson. *Sliding Friction: Physical Principles and Applications.* Springer, Berlin, 1998.

[3] J. Krim. Friction at the atomic scale. *Scientific American*, pages 48–56, Oct 1996.

[4] C. Lu and A. Czanderna, editors. *Applications of Piezoelectric Quartz Crystal Microbalances.* Elsevier, Amsterdam, 1984.

[5] A. Widom and J. Krim. Q factors of quartz oscillator modes as a probe of submonolayer-film dynamics. *Phys. Rev. B*, 34(2):1403–1404, Jul 1986.

[6] J. Krim and A. Widom. Damping of a crystal oscillator by an adsorbed monolayer and its relation to interfacial viscosity. *Phys. Rev. B*, 38(17):12184–12189, Dec 1988.

[7] J. B. Sokoloff, J. Krim, and A. Widom. Determination of an atomic-scale frictional force law through quartz-crystal microbalance measurements. *Phys. Rev. B*, 48(12):9134–9137, Sep 1993.

[8] M. O. Robbins and M. H. Műser. Computer simulations of friction, lubrication and wear. Cond-mat/0001056, Jan 2000.

[9] B. N. J. Persson. Surface resistivity and vibrational damping in adsorbed layers. *Phys. Rev. B*, 44(7):3277–3296, Aug 1991.

[10] B. N. J. Persson and A. I. Volokitin. Electronic and phononic friction. In B. N. J. Persson and E. Tosatti, editors, *Physics of Sliding Friction*, NATO ASI Series, pages 253–264. Kluwer Academic Publishers, 1996.

[11] R. G. Tobin. Comment on "Surface resistivity and vibrational damping in adsorbed layers". *Phys. Rev. B*, 48(20):15468–15470, Nov 1993.

[12] B. N. J. Persson. Reply to "Comment on 'Surface resistivity and vibrational damping in adsorbed layers' ". *Phys. Rev. B*, 48(20):15471, Nov 1993.

[13] J. B. Sokoloff. Theory of the contribution to sliding friction from electronic excitations in the microbalance experiment. *Phys. Rev. B*, 52(7):5318–5322, Aug 1995.

[14] A. Dayo, W. Alnasrallah, and J. Krim. Superconductivity-dependent sliding friction. *Phys. Rev. Lett.*, 80(8):1690–1693, Feb 1998.

[15] B. N. J. Persson and E. Tosatti. The puzzling collapse of electronic sliding friction on a super-conductor surface. *Surface Science*, 411(1–2):855–857, Aug 1998.

[16] R. L. Renner, J. E. Rutledge, and P. Taborek. Quartz microbalance studies of superconductivity-dependent sliding friction. *Phys. Rev. Lett.*, 83(6):1261, Aug 1999.

[17] B. N. J. Persson and R. Rydberg. Brownian motion and vibrational phase relaxation at surfaces: CO on Ni(111). *Phys. Rev. B*, 32(6):3586–3596, Sep 1985.

[18] Y. Georgievskii, M. A. Kozhushner, and E. Pollak. Activated surface diffusion: Are correlated hops the rule or the exception? *J. Chem. Phys.*, 102(17):6908–6918, May 1995.

[19] Ernst Schmutzer and Jerzy Plebański. Quantum mechanics in non-inertial frames of reference. *Fortschritte der Physik*, 25(1):37–82, 1977.

[20] S. V. Vonsovsky and M. I. Katsnelson. *Quantum Solid-State Physics*, volume 73 of *Solid-State Sciences*. Springer, 1989. Sec. 4.4.3, pages 316–319.

[21] E. N. Economou. *Green's Functions in Quantum Physics*, volume 7 of *Solid-State Sciences*. Springer, second edition, 1990.

[22] J. A. Hudson. *The excitation and propagation of elastic waves*. Mechanics and Applied Mathematics. Cambridge University Press, 1980.

[23] Ke-Hsueh Li. Physics of open systems. *Physics Reports*, 134(1):1, 1986.

[24] R. Kubo, M. Toda, and N. Hashitsume. *Statistical Physics II - Nonequilibrium Statistical Mechanics*, volume 31 of *Solid-State Sciences*. Springer, second edition, 1991.

[25] G. D. Mahan. *Many-Particle Physics*. Plenum, New York, second edition, 1990.

[26] M. S. Tomassone and A. Widom. Electronic friction forces on molecules moving near metals. *Phys. Rev. B*, 56(8):4938–4943, Aug 1997.

[27] W. L. Schaich. Brownian motion friction parameter of an ion near a metal surface. *Solid State Communications*, 15:357–360, 1974.

[28] T. L. Ferrell, P. M. Echenique, and R. H. Ritchie. Friction parameter of an ion near a metal surface. *Solid State Communications*, 32:419–422, 1979.

[29] A. Liebsch. Density-functional calculation of electronic friction of ions and atoms on metal surfaces. *Phys. Rev. B*, 55(19):13263–13273, May 1997.

[30] T. Novotný and B. Velický. Electronic sliding friction of atoms physisorbed at superconductor surface. *Phys. Rev. Lett.*, 83(20):4112–4115, Nov 1999.

[31] J. B. Sokoloff, M. S. Tomassone, and A. Widom. Strongly temperature dependent sliding friction for a superconducting interface. *Phys. Rev. Lett.*, 84(3):515–517, Jan 2000.

[32] B. N. J. Persson and E. Zaremba. Electron-hole pair production at metal surfaces. *Phys. Rev. B*, 31(4):1863–1872, Feb 1985.

[33] J. F. Annett and P. M. Echenique. Long-range excitation of electron-hole pairs in atom-surface scattering. *Phys. Rev. B*, 36(17):8986–8991, Dec 1987.

[34] P. M. Echenique, R. H. Ritchie, N. Barberán, and J. Inkson. Semiclassical image potential at a solid surface. *Phys. Rev. B*, 23(12):6486–6493, 1981.

[35] L. S. Levitov. Van der Waals' friction. *Europhysics Letters*, 8(6):499–504, Mar 1989.

[36] J. B. Pendry. Shearing the vacuum – quantum friction. *J. Phys. Condens. Matter*, (9):10301, 1997.

[37] B. N. J. Persson and Zhenyu Zhang. Theory of friction: Coulomb drag between two closely spaced solids. *Phys. Rev. B*, 57(12):7327–7334, Mar 1998.

[38] A. I. Volokitin and B. N. J. Persson. Theory of friction: the contribution from a fluctuating electromagnetic field. *J. Phys.: Condens. Matter*, (11):345–359, Jan 1999.

[39] B. N. J. Persson and A. I. Volokitin. Electronic friction of physisorbed molecules. *J. Chem. Phys.*, 103(19):8679–8683, Nov 1995.

[40] V. L. Popov. Electronic contribution to sliding friction in normal and superconducting states. *JETP Letters*, 69(7):558–561, Apr 1999.

[41] P. G. de Gennes. *Superconductivity of metals and alloys*. Benjamin, New York, 1966.

[42] J. R. Schrieffer. *Theory of superconductivity*. Benjamin, New York, 1965.

[43] B. N. J. Persson. Electronic friction on a superconductor surface. Preprint, Dec 1999.

[44] C. R. Doering and J. C. Gadoua. Resonant activation over a fluctuating barrier. *Phys. Rev. Lett.*, 69(16):2318–2321, Oct 1992.

[45] P. Reimann and P. Hănggi. Surmounting fluctuating barriers: Basic concepts and results. In L. Schimansky-Geier and T. Pőschel, editors, *Stochastic Dynamics*, number 484 in Lecture Notes in Physics, pages 127–139. Springer, Berlin, 1997.

[46] U. Zűrcher and C. R. Doering. Thermally activated escape over fluctuating barriers. *Phys. Rev. E*, 47(6):3862–3869, Jun 1993.

[47] M. Gitterman, R. I. Shrager, and G. H. Weiss. Stochastic resonance and symmetry breaking in a one-dimensional system. *Phys. Rev. E*, 56(3):3713–3716, Sep 1997.

[48] P. Chvosta and N. Pottier. Boundary problems for diffusion in a fluctuating potential. *Physica A*, 255:332–346, 1998.

[49] J. M. Porra. When coherent stochastic resonance appears. *Phys. Rev. E*, 55(6):6533–6539, Jun 1997.

[50] A. K. Dhara and T. Mukhopadhyay. Coherent stochastic resonance in the case of two absorbing boundaries. *Phys. Rev. E*, 60(3):2727–2736, Sep 1999.

[51] A. K. Dhara and S. R. Banerjee. Features of first passage time density function for coherent stochastic resonance in the case of two absorbing boundaries. Cond-mat/0002223, Feb 2000.

[52] P. Chvosta and P. Reineker. Dynamics under the influence of semi-markov noise. *Physica A*, 268:103, 1999.

[53] J. Klafter, M. F. Shlesinger, and G. Zumofen. Beyond Brownian motion. *Physics Today*, pages 33–39, Feb 1996.

[54] E. Barkai and V. N. Fleurov. Lévy walks and generalized stochastic collision models. *Phys. Rev. E*, 56(6):6355–6361, Dec 1997.

[55] E. Barkai and V. N. Fleurov. Generalized Einstein relation: A stochastic modeling approach. *Phys. Rev. E*, 58(2):1296–1310, Aug 1998.

[56] F. García-Moliner and V. R. Velasco. *Theory of Single and Multiple Interfaces*. World Scientific, Singapore, 1992.

# Appendix A

# Phononic Green's function for the half-space

In this appendix, we will calculate the *retarded* Green's function given by the equation (2.43).[1] As was already mentioned in the main text, this task separates into two independent problems. The first one is to find the scalar Green's function $G_{11}(z;z',\kappa,\omega)$ from the equation

$$\mu\Big(\frac{d^2}{dz^2}+q_T^2\Big)G_{11}(z;z',\kappa,\omega)=\delta(z-z') \tag{A.1}$$

with the boundary condition

$$\frac{d}{dz}G_{11}(z;z',\kappa,\omega)\Big|_{z=0}=0\ , \tag{A.2}$$

while the second part consists in finding the matrix Green's function $\left(\begin{smallmatrix}G_{22} & G_{23}\\ G_{32} & G_{33}\end{smallmatrix}\right)(z;z',\kappa,\omega)$ satisfying

$$\begin{pmatrix} \mu\frac{d^2}{dz^2}+\Gamma q_L^2 & i\kappa(\Gamma-\mu)\frac{d}{dz}\\ i\kappa(\Gamma-\mu)\frac{d}{dz} & \Gamma\frac{d^2}{dz^2}+\mu q_T^2\end{pmatrix}\cdot\begin{pmatrix} G_{22} & G_{23}\\ G_{32} & G_{33}\end{pmatrix}(z;z',\kappa,\omega)=\delta(z-z')\begin{pmatrix}1&0\\0&1\end{pmatrix} \tag{A.3}$$

with the boundary condition written in the matrix form as

$$\frac{d}{dz}\begin{pmatrix} G_{22} & G_{23}\\ G_{32} & G_{33}\end{pmatrix}(z;z',\kappa,\omega)\Big|_{z=0}=-i\kappa\begin{pmatrix}0&1\\ \frac{\lambda}{\Gamma}&0\end{pmatrix}\cdot\begin{pmatrix} G_{22} & G_{23}\\ G_{32} & G_{33}\end{pmatrix}(0;z',\kappa,\omega)\ , \tag{A.4}$$

which may be rewritten into the homogeneous matrix "reflecting" condition

$$\begin{pmatrix}\frac{d}{dz}&i\kappa\\ i\kappa\frac{\lambda}{\Gamma}&\frac{d}{dz}\end{pmatrix}\cdot\begin{pmatrix} G_{22} & G_{23}\\ G_{32} & G_{33}\end{pmatrix}(z;z',\kappa,\omega)\Big|_{z=0}=\mathcal{R}\mathbf{G}(z;z',\kappa,\omega)|_{z=0}=\mathbf{0}\,. \tag{A.5}$$

[1] In this appendix, we will omit the superscript $R$ denoting that the Green's function is retarded.

In the second part of this equation, we introduced the shorthand notation for the application of the reflecting boundary condition operator $\mathcal{R} = \left(\begin{smallmatrix} \frac{d}{dz} & i\kappa \\ i\kappa\frac{\lambda}{\Gamma} & \frac{d}{dz} \end{smallmatrix}\right)$ to the whole matrix Green's function denoted by $\mathbf{G}(z; z'\kappa, \omega)$. Even though both these quantities exist independently of each other, in the next we will always use the reflection boundary condition operator in the connection with the Green's function as shown above. We recall here that $\Gamma = \lambda + 2\mu$ ($\lambda$, $\mu$ are the Lamé coefficients) and

$$q_L^2 = \frac{(\omega + i\epsilon)^2}{c_L^2} - \kappa^2 = \frac{\omega^2}{c_L^2} - \kappa^2 + i\epsilon\,\mathrm{sign}\omega\,, \tag{A.6a}$$

$$q_T^2 = \frac{(\omega + i\epsilon)^2}{c_T^2} - \kappa^2 = \frac{\omega^2}{c_T^2} - \kappa^2 + i\epsilon\,\mathrm{sign}\omega \tag{A.6b}$$

with $c_L = \sqrt{\frac{\Gamma}{\varrho}}$ and $c_T = \sqrt{\frac{\mu}{\varrho}}$.

We will solve these two equations in the halfspace $z, z' < 0$ and the "reflecting" boundary conditions (A.2) and (A.5) should be understood as limits $z \to 0^-$. Both the problems introduced above are standard in the context of the surface Green's functions method [56]. They can be solved straightforwardly by applying the methods developed in detail in the textbook [56]. However, in this presentation we will illustrate the standard method only in the solution of the scalar equation, while in the second problem we will use a tricky shortcut approach which saves a big deal of work.

Let us now solve the equation (A.1) with the boundary condition (A.2), using the standard method. That is, we find two independent solutions of the homogeneous equation

$$\mu\Big(\frac{d^2}{dz^2} + q_T^2\Big) u_{\gtrless}(z; \kappa, \omega) = 0\ , \tag{A.7}$$

satisfying the boundary condition $\frac{du_>(z)}{dz} = 0$ at $z = 0$ and the natural boundary condition at $z \to -\infty$ reading $\lim_{z\to-\infty} u_<(z) = 0$, respectively. Since the regularization depends on $\mathrm{sign}\omega$, we will explicitly perform the derivation for the $\omega > 0$ case only. The opposite case is done analogously. Thus, for $\omega > 0$ we get the two solutions satisfying the homogeneous equation with the respective boundary conditions

$$u_<(z) \propto e^{-iq_T z} \text{ and } u_>(z) \propto \cos(q_T z) \tag{A.8}$$

with $q_T = \sqrt{\frac{\omega^2}{c_T^2} - \kappa^2} + i\epsilon$ when $\omega \geq c_T\kappa$ and $q_T = i\sqrt{\kappa^2 - \frac{\omega^2}{c_T^2}}$ when $\omega \leq c_T\kappa$. The Green's function $G_{11}(z; z')$ may be composed of these homogeneous solutions in the following way ([56], Chap. 1.1)

$$G_{11}(z; z') = C \begin{cases} u_<(z)u_>(z') & z \leq z'\ , \\ u_<(z')u_>(z) & z' \leq z\ . \end{cases} \tag{A.9}$$

This form of the Green's function ensures the continuity of $G_{11}(z;z')$ at $z=z'$ and also that it satisfies both the boundary conditions. The only unknown parameter, the constant $C$, is found readily by imposing the jump condition

$$\lim_{z\to z'+0}\frac{dG_{11}(z;z')}{dz}-\lim_{z\to z'-0}\frac{dG_{11}(z;z')}{dz}=\frac{1}{\mu}\,, \tag{A.10}$$

which is a consequence of (A.1) on $G_{11}(z;z')$ introduced above. The final equation for $C$ contains the Wronskian of the two solutions of the homogeneous equation, which is a non-zero constant (independent of the evaluation point $z'$), and, thus, we see that we get a unique solution to our problem. Performing the analogous procedure also for the $\omega<0$ case, we come to the final result for $G_{11}(z;z')$

$$G_{11}(z;z')=\frac{\mathrm{sign}\omega}{2i\,\mu q_T}\Big(e^{iq_T\mathrm{sign}\omega|z-z'|}+e^{-iq_T\mathrm{sign}\omega(z+z')}\Big)\,. \tag{A.11}$$

This was the illustration of the standard method found in textbooks. Even in this simple scalar case, we met quite extensive calculations mainly due to the fact that two cases $\omega\gtrless 0$ had to be distinguished. In the matrix case, one must use even more complicated matching ansatz analogous to (A.9) (cf. [56]), and the analogous calculations start being enormous. It is therefore convenient to use the shortcut approach introduced in the next. It utilizes the tricky ansatz which states the Green's function satisfying the boundary condition (A.5) in terms of the Green's function in the unrestricted 1D space satisfying the natural boundary conditions in $\pm\infty$. The same tricky approach may be successfully used in the scalar case, yielding the same result as the one obtained above. A reader may decide, whether this tricky approach is more convenient in that case. It is definitely much more effective in the matrix case which we will deal with now.

We can easily express the matrix Green's function $\left(\begin{smallmatrix}G_{22}&G_{23}\\G_{32}&G_{33}\end{smallmatrix}\right)(z;z',\kappa,\omega)$ using the Green's function of the equation (A.3) in the unrestricted space denoted by $\mathbf{G}_0(z;z')\equiv\mathbf{G}_0(z-z')$. Namely,

$$\mathbf{G}(z;z',\kappa,\omega)\equiv\mathbf{G}(z;z')=\mathbf{G}_0(z;z')-\mathbf{G}_0(z;0)\cdot\big[\mathcal{R}\mathbf{G}_0(0^-;0)\big]^{-1}\cdot\mathcal{R}\mathbf{G}_0(0;z')\,,\quad z,z'<0\,. \tag{A.12}$$

One can easily see that $\mathbf{G}(z,z')$ expressed in this way is really the Green's function of the equation (A.3) and that it satisfies the required boundary condition (A.5). The second term acts as a homogeneous solution to (A.3) in $z<0$, while it ensures that the boundary condition is satisfied.

The Green's function $\mathbf{G}_0(z-z')$ may be evaluated easily by using the Fourier transform with respect to $z-z'$ defined as

$$\widetilde{\mathbf{G}}_0(k) = \int_{-\infty}^{\infty}d(z-z')e^{ik(z-z')}\mathbf{G}_0(z-z')\,, \tag{A.13a}$$

$$\mathbf{G}_0(z-z') = \int_{-\infty}^{\infty}\frac{dk}{2\pi}e^{-ik(z-z')}\widetilde{\mathbf{G}}_0(k)\,. \tag{A.13b}$$

Using the Fourier transform, we rewrite the defining equation for $\mathbf{G}_0(z-z')$ (Eq. (A.3) with the natural boundary conditions at $\pm\infty$) into a simple matrix equation for $\widetilde{\mathbf{G}}_0(k)$

$$\begin{pmatrix} \Gamma q_L^2 - \mu k^2 & \kappa(\Gamma-\mu)k \\ \kappa(\Gamma-\mu)k & \mu q_T^2 - \Gamma k^2 \end{pmatrix} \cdot \widetilde{\mathbf{G}}_0(k) = \mathbf{1}\,, \tag{A.14}$$

which is straightforwardly solved and yields

$$\widetilde{\mathbf{G}}_0(k) = \frac{1}{\mu\Gamma(k^2-q_L^2)(k^2-q_T^2)} \begin{pmatrix} \mu q_T^2 - \Gamma k^2 & -\kappa(\Gamma-\mu)k \\ -\kappa(\Gamma-\mu)k & \Gamma q_L^2 - \mu k^2 \end{pmatrix}. \tag{A.15}$$

Now, performing the inverse Fourier transform and taking into account the infinitesimal parts present in $q_{L,T}^2$ properly, we come to the final result for $\mathbf{G}_0(z-z')$

$$\begin{aligned} \mathbf{G}_0(z-z') = \frac{1}{2i\varrho\omega^2} \Bigg\{ & e^{iq_L \mathrm{sign}\omega|z-z'|} \begin{pmatrix} \frac{\kappa^2}{q_L}\,\mathrm{sign}\omega & \kappa\,\mathrm{sign}(z-z') \\ \kappa\,\mathrm{sign}(z-z') & q_L\,\mathrm{sign}\omega \end{pmatrix} \\ & + e^{iq_T \mathrm{sign}\omega|z-z'|} \begin{pmatrix} q_T\,\mathrm{sign}\omega & -\kappa\,\mathrm{sign}(z-z') \\ -\kappa\,\mathrm{sign}(z-z') & \frac{\kappa^2}{q_T}\,\mathrm{sign}\omega \end{pmatrix} \Bigg\}\,. \end{aligned} \tag{A.16}$$

Having obtained the Green's function in the unrestricted space, we may now use the equation (A.12) to calculate $\mathbf{G}(z;z')$. To this end, we need to know the quantity $\mathcal{R}\mathbf{G}_0(z;z')$ which reads

$$\begin{aligned} \mathcal{R}\mathbf{G}_0(z;z') &= \begin{pmatrix} \frac{d}{dz} & i\kappa \\ i\kappa\frac{\lambda}{\Gamma} & \frac{d}{dz} \end{pmatrix} \cdot \mathbf{G}_0(z;z') \\ &= \frac{1}{2\varrho\omega^2} \Bigg\{ e^{iq_L \mathrm{sign}\omega|z-z'|} \begin{pmatrix} 2\kappa^2\,\mathrm{sign}(z-z') & 2\kappa q_L\,\mathrm{sign}\omega \\ \frac{\kappa}{q_L}(q_L^2+\frac{\lambda}{\Gamma}\kappa^2)\,\mathrm{sign}\omega & (q_L^2+\frac{\lambda}{\Gamma}\kappa^2)\,\mathrm{sign}(z-z') \end{pmatrix} \\ &\quad + e^{iq_T \mathrm{sign}\omega|z-z'|} \begin{pmatrix} (q_T^2-\kappa^2)\,\mathrm{sign}(z-z') & -\frac{\kappa}{q_T}(q_T^2-\kappa^2)\,\mathrm{sign}\omega \\ q_T\kappa(\frac{\lambda}{\Gamma}-1)\,\mathrm{sign}\omega & \kappa^2(1-\frac{\lambda}{\Gamma})\,\mathrm{sign}(z-z') \end{pmatrix} \Bigg\}. \end{aligned} \tag{A.17}$$

This leads to the following expressions for $\mathcal{R}\mathbf{G}_0(0^-;0)$

$$\mathcal{R}\mathbf{G}_0(0^-;0) = \frac{1}{2\varrho\omega^2} \begin{pmatrix} -\frac{\omega^2}{c_T^2} & \frac{\kappa}{q_T}(\kappa^2-q_T^2+2q_Lq_T)\,\mathrm{sign}\omega \\ \kappa\big(q_T(\frac{\lambda}{\Gamma}-1)+q_L(1+\frac{\lambda}{\Gamma}\frac{\kappa^2}{q_L^2})\big)\,\mathrm{sign}\omega & -\frac{\omega^2}{c_L^2} \end{pmatrix} \tag{A.18}$$

and for $[\mathcal{R}\mathbf{G}_0(0^-;0)]^{-1}$

$$\big[\mathcal{R}\mathbf{G}_0(0^-;0)\big]^{-1} = -\frac{2\varrho\omega^2}{\mathrm{Det}}\mathbf{M}\,, \tag{A.19a}$$

where

$$\mathrm{Det} = \frac{\mu}{\Gamma}\kappa^4\Big(1+\frac{\kappa^2}{q_L q_T}\Big)\left[\Big(\frac{q_T^2}{\kappa^2}-1\Big)^2+\frac{4q_Lq_T}{\kappa^2}\right] \tag{A.19b}$$

and

$$\mathbf{M} = \begin{pmatrix} \frac{\omega^2}{c_L^2} & -\frac{\kappa}{q_T}\big(\frac{\omega^2}{c_T^2}-2(\kappa^2+q_Lq_T)\big)\,\mathrm{sign}\omega \\ \frac{\kappa}{q_L}\big(\frac{\omega^2}{c_L^2}-2\frac{\mu}{\Gamma}(\kappa^2+q_Lq_T)\big)\,\mathrm{sign}\omega & \frac{\omega^2}{c_T^2} \end{pmatrix}. \tag{A.19c}$$

To simplify the matrix multiplication involved in the equation (A.12), we will use the tensor decomposition of the projectors corresponding to the longitudinal or transverse modes in $\mathbf{G}_0(z;0)$ and $\mathcal{R}\mathbf{G}_0(0;z')$, respectively. Thus, $\mathbf{G}_0(z;0)$ and $\mathcal{R}\mathbf{G}_0(0;z')$ may be rewritten in the following forms

$$\begin{aligned}\mathbf{G}_0(z;0) = \frac{1}{2i\varrho\omega^2}\Bigg\{ & e^{-iq_Lz\,\mathrm{sign}\omega}\begin{pmatrix} -\frac{\kappa}{q_L}\,\mathrm{sign}\omega \\ 1\end{pmatrix}\otimes\begin{pmatrix} -\kappa & q_L\,\mathrm{sign}\omega\end{pmatrix} \\ & + e^{-iq_Tz\,\mathrm{sign}\omega}\begin{pmatrix} q_T\,\mathrm{sign}\omega \\ \kappa\end{pmatrix}\otimes\begin{pmatrix} 1 & \frac{\kappa}{q_T}\,\mathrm{sign}\omega\end{pmatrix}\Bigg\},\end{aligned} \tag{A.20}$$

$$\begin{aligned}\mathcal{R}\mathbf{G}_0(0;z') = \frac{1}{2\varrho\omega^2}\Bigg\{ & e^{-iq_Lz'\,\mathrm{sign}\omega}\begin{pmatrix} 2\kappa \\ \frac{\mathrm{sign}\omega}{q_L}(q_L^2+\frac{\lambda}{\Gamma}\kappa^2)\end{pmatrix}\otimes\begin{pmatrix} \kappa & q_L\,\mathrm{sign}\omega\end{pmatrix} \\ & + e^{-iq_Tz'\,\mathrm{sign}\omega}\begin{pmatrix} q_T^2-\kappa^2 \\ -\frac{2\mu}{\Gamma}q_T\kappa\,\mathrm{sign}\omega\end{pmatrix}\otimes\begin{pmatrix} 1 & -\frac{\kappa}{q_T}\,\mathrm{sign}\omega\end{pmatrix}\Bigg\}.\end{aligned} \tag{A.21}$$

Using these expressions in (A.12), we come to the result

$$\begin{aligned}\begin{pmatrix} G_{22} & G_{23} \\ G_{32} & G_{33}\end{pmatrix}(z;z',\kappa,\omega) = \frac{1}{2i\varrho\omega^2}\Bigg\{ & e^{iq_L\,\mathrm{sign}\omega|z-z'|}\begin{pmatrix} \frac{\kappa^2}{q_L}\,\mathrm{sign}\omega & \kappa\,\mathrm{sign}(z-z') \\ \kappa\,\mathrm{sign}(z-z') & q_L\,\mathrm{sign}\omega\end{pmatrix} \\ & + e^{iq_T\,\mathrm{sign}\omega|z-z'|}\begin{pmatrix} q_T\,\mathrm{sign}\omega & -\kappa\,\mathrm{sign}(z-z') \\ -\kappa\,\mathrm{sign}(z-z') & \frac{\kappa^2}{q_T}\,\mathrm{sign}\omega\end{pmatrix} \\ & + e^{-iq_L\,\mathrm{sign}\omega(z+z')}\,R_{LL}\begin{pmatrix} -\frac{\kappa^2}{q_L}\,\mathrm{sign}\omega & -\kappa \\ \kappa & q_L\,\mathrm{sign}\omega\end{pmatrix} \\ & + e^{-iq_T\,\mathrm{sign}\omega(z+z')}\,R_{TT}\begin{pmatrix} q_T\,\mathrm{sign}\omega & -\kappa \\ \kappa & -\frac{\kappa^2}{q_T}\,\mathrm{sign}\omega\end{pmatrix} \\ & + e^{-i\,\mathrm{sign}\omega(q_Lz+q_Tz')}\,R_{LT}\begin{pmatrix} q_T\,\mathrm{sign}\omega & -\kappa \\ -\frac{q_Lq_T}{\kappa} & q_L\,\mathrm{sign}\omega\end{pmatrix} \\ & + e^{-i\,\mathrm{sign}\omega(q_Tz+q_Lz')}\,R_{TL}\begin{pmatrix} q_T\,\mathrm{sign}\omega & \frac{q_Lq_T}{\kappa} \\ \kappa & q_L\,\mathrm{sign}\omega\end{pmatrix}\Bigg\},\end{aligned} \tag{A.22a}$$

where the respective reflection coefficients are given by

$$R_{LL} = \frac{1}{\mathrm{Det}} \begin{pmatrix} -\kappa & q_L \,\mathrm{sign}\omega \end{pmatrix} \cdot \mathbf{M} \cdot \begin{pmatrix} 2\kappa \\ \frac{\mathrm{sign}\omega}{q_L}(q_L^2 + \frac{\lambda}{\Gamma}\kappa^2) \end{pmatrix} , \tag{A.22b}$$

$$R_{TT} = \frac{1}{\mathrm{Det}} \begin{pmatrix} 1 & \frac{\kappa}{q_T}\,\mathrm{sign}\omega \end{pmatrix} \cdot \mathbf{M} \cdot \begin{pmatrix} q_T^2 - \kappa^2 \\ -\frac{2\mu}{\Gamma} q_T \kappa \,\mathrm{sign}\omega \end{pmatrix} , \tag{A.22c}$$

$$R_{LT} = -\frac{\kappa}{q_L q_T \mathrm{Det}} \begin{pmatrix} -\kappa & q_L \,\mathrm{sign}\omega \end{pmatrix} \cdot \mathbf{M} \cdot \begin{pmatrix} q_T^2 - \kappa^2 \\ -\frac{2\mu}{\Gamma} q_T \kappa \,\mathrm{sign}\omega \end{pmatrix} , \tag{A.22d}$$

$$R_{TL} = \frac{\kappa}{\mathrm{Det}} \begin{pmatrix} 1 & \frac{\kappa}{q_T}\,\mathrm{sign}\omega \end{pmatrix} \cdot \mathbf{M} \cdot \begin{pmatrix} 2\kappa \\ \frac{\mathrm{sign}\omega}{q_L}(q_L^2 + \frac{\lambda}{\Gamma}\kappa^2) \end{pmatrix} . \tag{A.22e}$$

With the help of the relations

$$\begin{pmatrix} -\kappa & q_L \,\mathrm{sign}\omega \end{pmatrix} \cdot \mathbf{M} = \Big(1 + \frac{\kappa^2}{q_L q_T}\Big) \begin{pmatrix} -2\frac{\mu}{\Gamma}\kappa q_L q_T & q_L(q_T^2 - \kappa^2)\mathrm{sign}\omega \end{pmatrix} , \tag{A.23a}$$

$$\begin{pmatrix} 1 & \frac{\kappa}{q_T}\,\mathrm{sign}\omega \end{pmatrix} \cdot \mathbf{M} = \Big(1 + \frac{\kappa^2}{q_L q_T}\Big) \begin{pmatrix} \frac{\mu}{\Gamma}(q_T^2 - \kappa^2) & 2\kappa q_L \mathrm{sign}\omega \end{pmatrix} , \tag{A.23b}$$

we obtain the final results

$$R_{LL} = R_{TT} = \frac{\Big(\frac{q_T^2}{\kappa^2} - 1\Big)^2 - 4\frac{q_L q_T}{\kappa^2}}{\Big(\frac{q_T^2}{\kappa^2} - 1\Big)^2 + 4\frac{q_L q_T}{\kappa^2}} , \tag{A.24a}$$

$$R_{LT} = R_{TL} = 4\frac{\frac{q_T^2}{\kappa^2} - 1}{\Big(\frac{q_T^2}{\kappa^2} - 1\Big)^2 + 4\frac{q_L q_T}{\kappa^2}} . \tag{A.24b}$$

# Appendix B

# Electronic Sliding Friction of Atoms Physisorbed at Superconductor Surface

Tomáš Novotný and Bedřich Velický

*Phys. Rev. Lett.*, 83(20):4112–4115, Nov 1999

# Appendix C

# Resonant Activation Phenomenon for Non-Markovian Potential-Fluctuation Processes

Tomáš Novotný and Petr Chvosta

Submitted to *Phys. Rev. E*, cond-mat/0004351, Apr 2000